جمهورية العراق
وزارة التعليم العـالي والبحث العلـمي
جامـــعة بـــابـــل
كليـــة العلـوم للبنات
قســـم فيزيـــاء الليزر

الخصائص الالكتروضوئية والحرارية للوصلات الجزيئية النانوية

أطروحة قدمتها
الى مجلس كلية العلوم للبنات في جامعة بابل
وهي جزءً من متطلبات نيل درجة الدكتوراه فلسفة
في العلوم/ فيزياء الليزر وتطبيقاته

من قبل الطالبة

زينب عبد الزهرة عبد الحسن

بكالوريوس في علوم فيزياء الليزر جامعة بابل **(2012)**
ماجستير في علوم فيزياء الليزر جامعة بابل **(2016)**

بأشراف

أ. د. ايناس محمد الربيعي

كلية العلوم للبنات/ قسم فيزياء الليزر

2022 م **1443هـ**

Republic of Iraq
Ministry of Higher Education and Scientific Research
University of Babylon
College of Sciences for Women
Department of Laser Physics

Optoelectronic and Thermoelectric Properties of Nano Molecular Junctions

A Thesis

Submitted to the Council of the College of Sciences for Women, University of Babylon

In Partial Fulfillment of the Requirements for the Degree of Doctor of Philosophy in Laser Physics and its Applications

By

Zainab Abdul-Zahra Abdul-Hassan

B.Sc., Laser Physics and its Applications, University of Babylon (2012)
M.Sc., Laser Physics and its Applications, University of Babylon(2016)

Supervised by

Prof. Dr. Enas Mohammed AL-Robayi

University of Babylon
College of Science for Women
Laser Physics Department

1443 A.H. **2022 A.D.**

Dedication

I dedicate this thesis to my father,

Who always dreams of obtaining a Ph.D.

ACKNOWLEDGMENT

Above all, my great thanks are to **ALLAH** for his mercy and blessing.

This thesis would never completed without the excellent supervision and guidance I received from Prof. Dr. ***Enas M. AL-Robayi***. There are no words in English to express my gratitude to you. Really you are excellent supervisor.

I am deeply indebted to the Head of the Laser Physics Department, the Science for Women for the staff and the dean of the College of support that provided.

Also, I would like to pay my regards to all relatives and friends for the help they showed at the Department of Laser Physics.

I would like to express my very deep respect and sincere appreciation to my family, whose patience and moral encouragement gave me so much hope and support.

Zainab

الخلاصة :

يهدف مجال تقنية النانو إلى جعل المكونات الإلكترونية أصغر وأصغر ، مما يؤدي في النهاية إلى تحقيق أقل طول جزيئي مايقارب 2 نانومتر. الهدف من هذه الأطروحة فهم هذه المكونات من خلال دراسة الخصائص التركيبية والإلكترونية والبصرية والكهروحرارية لنظام يحتوي على اقطاب معدنية مرتبطة بجزيء مفردة. الجانب النظري المستخدم هو مزيج من نظرية الكثافة الوظيفية ونظرية غرين للتوازن التشتت.

لقد تم دراسة الخصائص التركيبية لمجموعتين من BDC ، باستخدام استراتيجية زيادة الطول الجزيئي لكلا المجموعتين.تمت زيادة الطول الجزيئي للمجموعة B بتكرار الوحدة الأساسية خمس مرات ، والتي حصلنا منها على خمسة جزيئات من مركبات BDC_B. أما بالنسبة للمجموعة (N) فقد تمت زيادة الطول بتكرار الوحدة الأساسية وكذلك عدد ذرات الكربون التي تشكل العمود الفقري للجزيء التي تتكون من ذرتين إلى أربع ذرات كربون. كان أقصر طول جزيئي (2 نانومتر) ، والذي تم الحصول عليه من الجزيء (1N). اما أطول طول جزيئي كان (5.9 نانومتر) ، والذي تم الحصول علية بواسطة الجزيء (5N). تم حساب جميع الاجزاء التركيبية الأخرى لجميع الجزيئات مثل الاواصر أحادية الكربون والكربون (C – C = 0.135 نانومتر) ، وطول الاصرة (X = 0.21 نانومتر) ، والمسافة النظرية بين الاقطاب (Z) ، هذا في الطور الغازي وبعد تشكيل الوصلة الجزيئية. أظهرت هذه الأطروحة أن هناك تأثيرًا مهمًا للطول الجزيئي والجوانب التركيبية الأخرى على الخواص الإلكترونية والبصرية والكهروحرارية.

الخصائص الإلكترونية والبصرية والكهربائية مثل توزيع المدارات الجزيئية وفجوات HOMO-LUMO ومعامل النقل وقوة المذبذب وطيف الأشعة فوق البنفسجية والموصلية الكهربائية والطاقة الحرارية وغير ذلك.

أظهرت الحسابات الإلكترونية أن آلية نقل حاملات الشحنة في هذا النوع من الجزيئات هي آلية النقل التي يهيمن عليها HOMO. يمكن رؤية نتيجة مهمة أن الطول الجزيئي لم يؤثر فقط على معامل النقل والتوصيل الكهربائي ولكن أيضًا خلق تأثير الحجم الكمي ، مما أثر على فجوة HOMO-LUMO. يملك أقصر طول جزيئي (1N) على أعلى موصلية كهربائية (0.27) وأوسع فجوة HOMO-LUMO

(2.51 Ev). حيث يتم الحصورعلى أقل توصيلية كهربائية (0.07) وأضيق فجوة (1.241 فولت) بواسطة أطول طول جزيئي للوصلة الجزيئية (5N).

نلاحظ أيضًا للمجموعتين (BDC_N) و (BDC_B) أنه مع زيادة الطول الجزيئي تزداد قوة المذبذب وهذا يرجع إلى تأثير الحجم الكم.

بالنسبة للخصائص الكهروحرارية للمجموعة (BDC_N) ، تمت دراسة معامل سيبيك S وشكل الجدارة ZT. أظهرت النتائج أن معامل سيبيك S لجميع المركبات هو موجب حيث اكدت هذه النتائج بأن آلية النقل المهيمنة هي HOMO. علاوة على ذلك ، قدمت هذه النتائج فكرة ممتازة لتصميم الأجهزة الحرارية الجزيئية. يعطي الطول الجزيئي الأطول (5N) أعلى قوة حرارية ($0.25*10^{-3}\ VK^{-1}$). بينما يظهر الجزيء الأقصر (1N) أقل مقاومة حرارية ($0.90*10^{-3}\ VK^{-1}$)

قدمت نتائج هذا العمل استراتيجية مثيرة للاهتمام لتعزيز رقم الجدارة (ZT) عن طريق زيادة عدد ذرات الكربون وتكرارات الوحدة الأساسية. حيث تم رفع قيمة ZT (من 0.3 إلى 4) بسبب الزيادة في الطول الجزيئي من 1N إلى 5N على التوالي.

وجدنا عند مقارنة المجموعتين (BDC_B) و (BDC_N) أن المجموعة (N) لها خصائص بصرية أفضل ، ولها قوة تذبذب أعلى من المجموعة (B) ، وهذا يجعلها مرشحًا واعدًا لاستخدامها كوسط فعال ليزري.

أخيرًا ، استنادًا إلى النتائج المقدمة في هذه الأطروحة ، يمكن أن تكون التراكيب والجزيئات التي تمت دراستها في هذا العمل مرشحة واعدة للتطبيق الواسع مثل الثنائيات الباعثة للضوء (LED) ، والترانزستورات ذات التأثير الميداني (FETs) ، والخلايا الشمسية ، وشاشات اللمس و اوساط ليزرية فعالة.

Abstract

The field of nanotechnology aims to make electronic components smaller and smaller, eventually achieving length scales of less than 2 nanometers. This thesis, aims to contribute to the understanding of these components by investigating the structural, electronic, optical and thermoelectric properties of a system containing metallic threads that are joined by a single molecule. The theoretical approach used is a combination of density functional theory and Greene's equilibrium dispersion theory of functions.

The structural properties of two groups of Binzodicollagenatphenon (BDC), using the strategy of increasing the molecular length of both groups,were investigated.

Group (B) the molecular length was increased by repeating the base unit for five times, from which we obtained five molecules of (BDC_B) compounds.

As for group (N), the length was increased by repeating the base unit, as well as the number of carbon atoms that form the backbone of the molecule from two to four carbon atoms.

Electronic, optical and electrical properties such as the distribution of molecular orbitals, highest occupied molecular orbitals (HOMO)- lowest unoccupied molecular orbitals (LUMO) gaps, transport coefficient, oscillator strength, UV spectrum, and thermoelectric properties.

The electronic calculations have demonstrated that the transport mechanism of charge carriers in this type of molecule is the transport mechanism dominated by HOMO. Importantly the molecular length not only affected the transport coefficient and electrical conductivity but also created

the quantum size effect, which affected the HOMO-LUMO gap. The shortest molecular length (1 N) has the highest electrical conductivity (0.27) and the widest HOMO-LUMO gap (2.51 eV). Whereas, the lowest conductivity (0.07) and the narrowest gap (1.241 eV) are presented by the longest molecular junction (5N).

The researcher also notice for the two groups (BDC_N) and (BDC_B) that with the increase in the molecular length, the oscillator strength increased and this is due to the effect of quantitative size.

For the group's thermoelectric properties (BDC_N), The researcher studied the Seebeck's coefficient S and the figure of merit (ZT). The results showed that the sign of Seebeck's coefficient S for all compounds is positive. These results supported the initial prediction that the transport mechanism is HOMO-controlled transport. Moreover, these results provided an excellent idea for the design of thermo-molecular devices.

The results of this work presented an interesting strategy to enhance the ZT by increasing the number of carbon atoms and base unit frequency.

When comparing the two groups (BDC_B) and (BDC_N), The researcher found that group (N) is better in terms of optical properties, as it has a higher oscillator strength than group (B), and this made it a promising candidate for using it as an effective laser medium.

Finally, based on the results presented in this thesis, the structures and molecules studied in this work can be promising candidates for wide application such as light-emitting diodes (LEDs), field-effect transistors (FETs), solar cells, and touch screens and laser active medium

List of Symbols

Symbol	Physical Meaning
G_+	(Advanced) Green's function
ε	Absorption intensity
$V_{nl}^{all-electron}$	All core-and valence-electron interactions
α	Alpha Carbon
Z	Atomic number
Ψ_v	Atomic orbitals
E_{Bin}	Binding energy
BDC	Binzodicollagenatphenon
K_B	Boltzmann constant
(C_4)	Butadiyne
j_{th}	Channel of the left lead
i_{th}	Channel of the right lead
I	Charge current
μ_L	Chemical potential in the left
μ_R	Chemical potential in the *right*
$\mathcal{G}$	Conductance

C_F	Constant Tomas-Fermi
r_c	Core radius
E_C	Correlation energy of an electron
$-\alpha$	Coupling element
$\partial n/\partial E$	Density of states (DOS) per unit length in the lead
ε_o	Dielectric constant of the vacuum
$s = \frac{\lvert V\rho \rvert}{2k_{F\rho}}$	Dimensionless density gradient
V_{eff}	Effective external potential
H_{eff}	Effective Hamiltonian
G/G0	Electrical conductance
e	Electron charge
E_{ele}	Electron energy
ZT_e	Electronic figure of merit
H_{ele}	Electronic Hamiltonian
$\boldsymbol{N}$	Electrons number
σ_{em}	Emission cross section
f_{em}	Emission oscillator strength
$F_{H-K}[n(\vec{r})]$	Energy functional of the Hohenberg-Kohn
$F_{K-S}[n(\vec{r})]$	Energy functional of the Kohn-Sham
E^A	Energy of the isolated subsystem A

E^B	Energy of the isolated subsystem B
$F_x(s)$	Enhancement factor
(C_2)	Ethyne
E_X	Exchange energy of an electron
E_{xc}	Exchange-correlation energy
$V_{ext}(\vec{r})$	External potential
f_L	Fermi distribution from the left
f_R	Fermi distribution from the right
f_i	Fermi distribution function
E_F	Fermi energy
$f(E)$	Fermi-Dirac function
n_{GS}	Ground state density
E_{GS}	Ground state energy
n(r)	Ground-state density
Ψ_{GS}	Ground-state wavefunctions
$\boldsymbol{v_g}$	Group velocity
H	Hamiltonian operator
Q	Heat current
$-\gamma$	Hopping parameters
δI^{in}	Incident electric current
U_{en}	Interaction between electrons and nuclei

U_{ee}	Interaction energy between all electrons
U_{nn}	Interaction energy terms between the nuclei
T_e	Kinetic energy for the electron
T_n	Kinetic energy for the nuclei
T_{int}	Kinetic energy of the interacting system
T_{non}	Kinetic energy of the non-interacting system
∇_i^2	Laplacian operator
$\Gamma_{L,R}(E)$	Level broadening due to the coupling between right (R) and left (L) electrodes
(C_0)	Linkers, or "fused"
r_s	Local Seitz radius
m_e	Mass of the electron
m_n	Mass of the nucleus
S	Matrix, it connects states coming from the left lead to the right lead and vice versa:
(=CH−)	methine bridges
φ_i	Molecular orbitals (basis functions)
Z_n	Nuclear charge
M	Nuclei number
a_{vi}	Numerical coefficients
E_i	Numerical value of the energy of the i^{th} state
ε_o	On-site energies

r	Outside of the core radius
ΔE_{inter}^{AB}	Overall energy of the supersystem
H	Planck's constant
r_i	Position of the electrons
r_i	Position of the *i-th* electron
R_I	Position of the I-th nucleus
R_I	Position of the nuclei
ΔV	Potential drop
R	Probability the reflection
T(E)	Probability the transition
V_{nl}^{ps}	Pseudo-potential
G_o	Quantum of conductance
R_{nl}^{ps}	Radial pseudo-wavefunction
R_{nl}^{I}	Radial wavefunction
$\overleftarrow{r}_{ij}$	Reflection amplitudes
$g(z, z')$	Retarded Green's function
G_-	Retarded Green's function
$\Psi_{nlm}^{I}(r)$	Single basis function
ε_1	Single site energy
$R_{nl}^{all-electron}$	Solution to the radial Schrödinger equation

Y_{lm}^{I}	Spherical harmonic
$\Delta\mathcal{T}$	Temperature
$\mathcal{T}_L$	Temperature left
$\mathcal{T}_R$	Temperature right
$S(T)$	Thermopower
k_{T-F}	Thomas-Fermi screening wavenumber
E_{total}	Total energy
E_a , E_d, E_e	Total energy of (a), (d) and (e) systems
L	Total number of the atomic orbitals
$\vec{t}_{ij}$	Transmission amplitude
E_{Tri}	Trial energy
Ψ_{Tri}	Trial wavefunctions
π-electrons	two electronic bonds
ε_2	Two site energy
δV	Voltage associated with the chemical potential mismatch
Ψ	Wave function
k	Wavenumber

List of Tables

1-1 Introduction

Nanoscale research and engineering enable revolutionary discoveries in both fundamental science and technology, which may have a direct impact on our daily lives. It is on a level with transistor-based electronics in terms of size and scope. At its most fundamental level, nanoscale science is the study of unique phenomena and properties of materials at extremely small length scales, namely at the nanoscale, which corresponds to the size of atoms and molecules [1].

The nanoscience revolution has emphasized the critical need for a more solid quantitative understanding of matter at the nanoscale through modeling and simulation, since the dearth of quantitative models that accurately characterize newly reported phenomena has stifled development in the area. Recently, fundamental modeling tools such as (DFT) and molecular dynamics have been used to gain new insights in the field of nanoscience [2]. Increased computing capabilities enabled the modeling and simulation of complex systems with millions of degrees of freedom as a result of advancements in computer technology. The entire promise of modern theoretical and modeling techniques, on the other hand, has not yet been realized [3].

Controlling individual molecules and their utilization is one of the scientific ambitions of our age. The realization of this ambition can open up broad prospects to a miniaturization revolution in electronic devices. In recent decades, developments in nanofabrication techniques have made achievable the dream of contacting individual molecules to nano-electrodes and measuring their electronic transport characteristics [4]. Moreover, molecules are highly desirable as functional elements in nano-scale devices

because of their ability to be chemically modified to tune their properties. Nowadays, these achievements have given rise to the field of molecular electronics.

1-2 Molecular electronics

Molecular electronics has attracted great attention from a wide variety of researchers, due to promising applications in nanoscale electronic devices such as transistors [5, 6], switches [7], rectifiers, interconnects [8], organic photovoltaic [9], and chemical sensors [10]. Using molecules as electronic elements has many advantages due to their small sizes, their ability to be self-assemble onto surfaces and the low cost of producing large numbers of identical molecules [11]. However, realizing and controlling the connection between the molecule and electrodes has remained challenging.

Due to small molecular size, The use of individual molecule as functional electronic devices was first proposed in the 1970`s [12]. In order to design and realize molecular devices it is essential to have a good understanding of the properties of an individual molecule. Within the framework of molecular electronics, the most important property of a molecules is:(the conductance and the major question in this field is how electrons move through molecules). To address this question, extensive experimental and theoretical studies have been carried out.. Various measurement techniques have been developed.

The concept of electrons passing through a single molecule comes via two different approaches [13]. Firstly, transfer of the electrons, which involves charge moving from one end of the molecule to the other. Secondly, transport of the charges, which involves current passing through

a single molecule that is connected between electrodes [14]. These two approaches are closely related, because both of them attempt to answer the previous question. From the point of view of fundamental science, molecular electronics could provide an answer for previous inquiry, and perhaps be an ideal way to explore the electronic and thermal conductance through the smallest molecular circuits, where quantum mechanical effects completely dominate [15].

The variety of molecules organic molecules, together with their various properties could lead to the discovery of new physical phenomena. In addition, molecular junctions could also be promising systems to investigate the basic principles of electron transfer mechanisms [16]. However, there are also other motivations in terms of a technological viewpoint, which is the use of molecules as electronically active elements for many applications. One of these reasons is the size, since the typical size of molecules (between 1 and 10 nm) it could lead to a higher packing density on a device with subsequent advantages in cost, efficiency and power dissipation These concepts and many others make molecular electronics an attractive field of science. Additionally, novel molecular phenomena such as quantum interference have been identified, opening up new avenues for molecular design and resulting in proposals for the design of molecular materials [17] with useful properties such as an enhanced thermoelectric figure of merit ZT and promisingly high-power factors GS^2 [18-19].

When a single molecule is linked to source and drain electrodes, the electrical conductance of the resulting device is controlled by the quantum interference pattern formed within the molecule by the source's de Broglie waves of electrons [20]. Motivated by the goal to increase the performance of molecular-scale diodes [21], transistors [22,23], switches [24], and

thermoelectric devices [25,26], current research has focused on harnessing such wave patterns within heterocyclic aromatic molecules.

In this thesis, it has focused on exploring the electronic, spectral, optical and thermoelectric properties of Binzodicollagenatphenon (BDC) Compound -based single molecule devices with different structural fathers. For this goal (BDC)-based molecular junctions are designed by contact the (BCD) molecules to two gold electrodes. Theoretically, three main techniques have been used to study the systems in this thesis; the first is the density functional theory (DFT), which is implemented in the SIESTA (Spanish Initiative for Electronic Simulations with Thousands of Atoms), and Gaussian codes [27,28]. The second one is the nonequilibrium Green's function formalism of transport theory, The three which is implemented in the GOLLUM code [29].

1-3 Binzodicollagenatphenon (BDC) Compound

Carbon-based on molecular junctions, such as carbon nanotubes [30] and graphene sheets [31], which have attracted a lot of interest as they represent promising candidates in the field of nanoelectronics. Nowadays, finding functional molecular wires that can connect molecular electronic devices is the main goal of many of investigations [32].

Bolycyclic hydrocarbons (PAH`s) and their derivatives are particularly attractive, as they contain multiple interference pathways, it can be influenced by external electrostatic or electrochemical gating [33], by changing their connections to external electrodes [34, 35] or by substitution heterogeneous atom [36].

In our work, we investigate the effect of the increase the molecular length when the parent is a non-binary aromatic molecule, catalyzed in part by a desire to understand electron transfer through (BDC) compounds.

The (BDC) compounds are rigid, planar π-conjugated structures, with molecular cores containing 5- membered rings fused to a 6-membered aryl ring Which Contains an S in one 5-membered ring and an (O) with the others [37-38], and a strong ability to electron donation [39, 40].

These properties have led to their use as organic electronic compounds in dye-sensitive solar cells (DSSC), field-effect transistors (FET), organic light-emitting diodes (OLED) and charge transfer studies of single molecules [41,42]. However, the non-binary nature of the central core, the irregular bonding geometry and the structural rearrangement of typical stabilization groups in the junction complicate the interpretation of the charge transfer data. The improvement was achieved using an alternative, highly conductive carbon-gold anchor using trimethylsilyl-terminated compounds, which facilitate interpretation of somewhat more robust data [43, 44].

One consequence of the large conjugate system is that BDC is typically strongly absorbed in the visible region of the electromagnetic spectrum. In other words, they are deeply colored [45]. An important topic that has received wide attention during the past years is the electronic, electrical and thermal properties of organic nanostructures and the relationship between them [46]. Nowadays, many researches focus and search for molecular wires that enable us to obtain optical and spectroscopic properties such as emission oscillator strength, excitation energies and molecular orbital character that can offer us promising active media for laser devices [47,48].

BDC represents one of the most studied classes of molecular wires in single-molecule electronics; therefore, porphyrin bands in the sense of π−π* energy gaps could be an ideal choice and play an important role in the development of organic optoelectronic applications[49, 50].

Seebeck coefficients and transition are the most important features of single molecular structures,and the search for ways to alter and control these properties becomes an attractive goal for many researchers.Therefore, in previous studies,these methods were used by molecular length change (BDC) method, probing the relationship [51] between electrical conductivity and thermal energy for BDC-based devices, which was a useful strategy for defining applications of these devices. and predict it. J. Song et. al. [52] mentioned the fact that the strength of the emission oscillator (f_{em}) is an important parameter for evaluating the performance of the effective medium of lasers [53].

Using the density functional theory (DFT) method [54-55], the strength of the emission oscillator can be obtained from calculations of electronic structures, thus serving as a rapid screening tool for optical gain materials. In this work, the number of (BDC) units and the number of backbone atoms of the molecule were altered in order to increase the molecular length and structural aspects [55]. Thesis contained not only the investigation of the effect for different structural features on the Seebeck and transmission coefficients, but also studied the effect of these features on the emission oscillator strength value [56,57].

1-4 Literature Survey

Molecular electronics is one of the most important fields of science that investigates the electronic transport and thermoelectric properties of structures in which a single molecule is utilized as a basic building blocks.

1- T. Markussen et al [58], in 2010, have proposed a simple and general graphical scheme which explains the strong relation between the structure of molecular junctions and the quantum interference effect.

2- A. Nataiya and R.Pederson [59], in 2011 gave an overview of the theoretical methods used to analyze the transport properties of the metal-molecular junctions in addition to some relevant experiments and applications.

3- P. Moreno-García et. al. [60], in 2013, have report a combined experimental and theoretical investigation of the length dependence and anchor group dependence of the electrical conductance of a series of oligoyne molecular wires in single-molecule junctions with gold contacts.

4- H. M. Wen et. al. [61] in 2013, reported the organometallic based molecular junctions that exhibit a high conductance compared with their organic analogous.

5- D.C.Milan et. al., [62] , in 2015, have shown not only the solvent environment but also which is a significant factor to consider in explaining the conductance properties of single molecule wires, but also it gives rise to remarkable alterations in attenuation factors.

6- A. Oday Al-Owaedi et. al. [57] , in 2016 , introduced a theoretical and experimental studies of trans-Ru complexes. They have interpreted the electronic properties of such molecules in terms of the transport mechanisms (LUMO-dominated conductance). These results have significant implications for the future design of organometallic complexes for studies in molecular junctions.

7- A. Oday Al-Owaedi et. al. [63] ,in 2017, present an investigation about the important role of the metal complexes inhibiting orthogonal contacts, which explained the strange high conductance values of some of organometallic molecules.

8- P. Sam-ang and G. R. Matthew, [64] in 2017 ,showed characterizing destructive quantum interference in electron transport. Destructive quantum interference in electron transport through molecules provides an unconventional route for suppressing electric current. In this work introduce interference vectors' for each interference and used them to characterize the interference. An interference vector may be a combination of multiple molecular orbitals (MOs), leading to more robust interference that is likelier to be experimentally observable.

9- R. J. Davidson et. al. [65], in 2018, to developed a new design of molecular nano junction depending on organometallic molecules. They explored the ability to control the orientation of molecular conductors on the electrode surfaces, which showed only a single high conductance feature.

10- C. J. Jud., [66], in 2020 , have measured the energetic and spatial distribution of the electronic states, by utilizing a combination of density functional theory and tight-binding calculations, they

interpret the experimentally obtained electronic structure in terms of coherent quantum states confined around the circumference of the π-conjugated macrocycle. These findings demonstrate that large (53 nm circumference) cyclic porphyrin polymers have the potential to act as molecular quantum rings.

11- A. A. Baraa Al-Mammory et. al. [67], in 2021, thermoelectric Properties of Oligoyne-Molecular Wires. Oligoynes are prototype molecular wires due to their conjugated system and the coherent tunneling transport, which aids this type of wires to transfer charges over long distances. The electric and thermoelectric characteristics for a series of Oligoyne molecular wires ((n) 3, 5, 7 and 9) are studied to explore the fundamental transport mechanisms for electrons crossing through single molecules, we probed both the electrical conductance and Seebeck coefficient for Au| molecule |Au configurations using (DFT).

12- M. Rasool Al-Utayjawee and **A. Oday Al-Owaedi,** [68], in 2021, Enhancement of Thermoelectric Properties of Porphyrinbased Molecular Junctions by Fano Resonances. Single-molecule porphyrin applications gain attention by using molecules as elementary blocks of electronic components involving metallic atoms. Theoretically, one type of molecular-scale porphyrin device is used in this article, consisting of organometallic single molecules with different metals (Zn, Mg, Cu and Fe), sandwiched between gold electrodes bound by thiol anchor groups. The transmission and Seebeck coefficients for (Au| molecule |Au) configurations were computed using (DFT).

13- **I. O. Abbas and M. Enas Al-Robayi**,[69], in 2022, Organometallic structures based on (BiCyclobentedine-metal-anchor groups) molecules can be potent devices for optoelectronics applications, notably for laser active mediums, because these structures introduced a high emission oscillator strength (f_{em}).

1-5 Amis of the Work

This research aims to investigate the electronic and thermoelectric properties of organic molecular junctions. Also, one of the main goals of this study is the exploring of some of optical characteristics such as HOMO-LUMO gap of these devices; Therefore, the goals of this work can be summarized as following:

1- It is improve and create active laser media that improve the efficiency an properties of laser devices through the use of molecules (Benzodichalcogenophene (BDC), where we use the strategy of change the length of the molecule and comparing them in terms of optical and structural properties.
2- Understand and study the optoelectronic and thermoelectric properties to predict the appropriate applications of these molecules in wide range of electronic and optoelectronic applications, such as organic solar cells, organic light-emitting diodes, organic field-effect transistors or active laser mediums.

2-1 Introduction

Quantum chemical calculations can assist researchers in designing and adapting target molecules while reducing the cost of tests. This is especially valuable for screening and monitoring high-energy materials (HEM). Molecular modeling is a collection of strategies for using a computer to examine chemical problems [70,71]. Clinicians and computational chemists can use one of four major approaches: Molecular Mechanics (MM), Semi-Empirical (SE), Ab initio, or Density Functional Theory (DFT) [72,73].

To predict the properties of the quantum mechanical system, an equation, describing how the wave function changes with time, is required. For one particle in one-dimensional system, this equation is the Schrödinger equation (Time dependent form) [74-75]:

$$i\hbar\frac{\partial}{\partial t}\Psi(\vec{r},t) = -\frac{\hbar^2}{2m}\nabla^2\Psi(\vec{r},t) + V(\vec{r})\Psi(\vec{r},t) = H(\vec{r},t)\Psi(\vec{r},t) \quad \text{.....(2.1)}$$

As

$$\hat{H}\,\Psi(\vec{r},t) = E\,\Psi(\vec{r},t) \quad \text{.....(2.2)}$$

Where $\hat{H}$ is the Hamiltonian operator, Ψ is the wave function and E is the system Eigen value. The Hamiltonian operator ($\hat{H}$) consists of two terms: the kinetic energy operator of the electrons and nuclei ($\hat{T}$) and potential energy components operator ($\hat{V}$), as follows:

$$\widehat{H} = \hat{T} + \hat{V} \quad \text{.....(2.3)}$$

The total Hamiltonian of the molecular system $\hat{H}$ containing M nuclei and N electrons can be expressed as follows [76,77]:

$$\hat{H} = \overbrace{-\frac{\hbar^2}{2m_i}\sum_{i=1}^{N}\nabla_i^2}^{electrons} - \overbrace{\frac{\hbar^2}{2M_A}\sum_{A=1}^{M}\nabla_A^2}^{nuclei} - \overbrace{\sum_{i=1}^{N}\sum_{A=1}^{M}\frac{Z_A}{r_{iA}}}^{electrons,nuclei} + \overbrace{\sum_{i=1}^{N}\sum_{j>i}^{N}\frac{1}{r_{ij}}}^{electrons} + \overbrace{\sum_{A=1}^{M}\sum_{B>A}^{M}\frac{Z_A Z_B}{r_{AB}}}^{nuclei} \quad \text{……..(2.4)}$$

Here ∇_i^2 is the Laplacian operator, in Cartesian coordinates is defined as:

$$\nabla_i^2 = \frac{\partial^2}{\partial x_i^2} + \frac{\partial^2}{\partial y_i^2} + \frac{\partial^2}{\partial z_i^2}$$

$$\hat{H}_{total} = \hat{T}_e + \hat{T}_n + \hat{V}_{ne} + \hat{V}_{ee} + \hat{V}_{nn} \quad \text{……..(2.5)}$$

The total kinetic energy is defined in equations (2.4) and (2.5) as the sum of the electronic ($\hat{T}_e$) and nuclear ($\hat{T}_n$) kinetic energies. The total potential energy is comprised of three components: attractive interactions between nuclei and electrons ($\hat{V}_{ne}$), repulsive interactions between nuclei ($\hat{V}_{nn}$), and repulsive electron-electron interactions ($\hat{V}_{ee}$). $Z_{A,B}$ denotes the nuclear charges of atoms A and B, respectively; m_A denotes the mass of atom A; r_{iA} denotes the distance between nucleus A and electron i, r_{AB} denotes the distance between nuclei A and B; and r_{ij} denotes the distance between i and j electrons, and $r_{ij} = |\vec{r}_i - \vec{r}_j|$.

The Born-Oppenheimer Approximation allows for the separation of electronic and nuclear motions in molecules. The molecule's entire wave function is as follows [72, 73, 77]:

$$\Psi_{total} = \Psi_{electronic} \times \Psi_{nuclear.} \quad \text{……..(2.6)}$$

Due to the fact that the nucleus is far heavier than electrons, nuclear motion is much slower than electronic motion. When the nucleus's kinetic energy is ignored, the nucleus's potential energy can be considered constant. Additionally, the Hamiltonian operator can be devoid of the nucleus's potential and kinetic energies. The Hamiltonian operator $\hat{H}$ can be expressed as follows:

$$\hat{H}_e=\hat{T}_e + \hat{V}_{ne} + \hat{V}_{ee} \quad \text{.....(2.7)}$$

2-2 Density Functional Theory

DFT is widely used by physicists and chemists to investigate the ground-state properties of interacting many-particles systems such as atoms, molecules and crystals [78]. DFT transforms many-body system into one of non-interacting fermions in an effective field. In other words, the electrical properties of many interacting particles system can be described as a functional of the ground-state density of the system [79].

In 1998 [80], the importance of DFT was confirmed with the Nobel Prize in Chemistry being awarded to Walter Kohn for his development of density functional theory. DFT is a reliable methodology which has been applied to a large variety of molecular systems with a huge number of books and articles in the literature giving detailed descriptions of the principles of DFT and its application [78-81]. The beginnings of DFT were founded upon the Thomas-Fermi model back in the 1920s [82] which provided the basic steps to obtain the density functional for the total energy based on wavefunctions [78,81,83]. Further improvement was made by Hartree, Dirac, Fock and Slater and nearly four decades after the Thomas-Fermi work. DFT was then given a robust foundation by the Hohenberg-Kohn theorems and Kohn-Sham method [80, 84].

The main aim of this chapter is to give brief introduction to DFT and outlining the main formalism as a method of finding the solution of the non-relativistic many-particles time independent Schrödinger equation TISE, since the properties of a many-electron system can be determined by using functionals of the electron density.

The researcher will also give a brief summary of the DFT code 'SIESTA', which has been used extensively throughout my PhD research as a theoretical tool to optimise the structures [83-85].

2-3 The Many-Body Problem

This is an approach which aims to solve any system consisting of a large number of interacting particles. In a microscopic system consisting of charged nuclei surrounded by electron clouds these interactions such as electron-nuclei, electron-electron, nuclei-nuclei and electron correlations are described via Schrödinger equation.

The full Hamiltonian operator of a general system describing these interactions is[86] :

$$H = \sum -\frac{\hbar 2}{2m_e}\nabla^2 + \frac{1}{8\pi\varepsilon_0}\sum_{n\to m}\frac{e^2}{|r_{n-}r_m|} - \sum_n \frac{\hbar 2}{2m_n}\nabla_{Rn}^2 + \frac{1}{8\pi\varepsilon_0}\sum_{n\to m}\frac{z_n - z_m\, e^2}{|R_N - R_M|} - \frac{1}{4\pi\epsilon_0}\frac{Z_e\, e^2}{|r_n - R_m|} \quad \ldots\ldots\ldots\ldots(2.8)$$

Here, m_n, Z_n and R_n represent the mass, atomic number and position of the *n-th* atom in the solid respectively. The position of *n-th* electron is denoted by the symbols rn,rm and me is the mass of a single electron. This Hamiltonian consists of five parts; the electron kinetic energy, electron-electron interactions, the nucleons kinetic energy, nucleon-nucleon interactions and electron-nucleon interactions respectively.

Approximately, the mass of nucleons is a few orders of magnitude higher than that of electron, and in terms of their velocities, the nuclei could be considered as a classical particle which creates an external potential, and the electrons as quantum particles are subjected to this potential [86].

I concept is known as the Born-Oppenheimer approximation [86], together with an assumption that the nucleon wavefunction is independent of the electron position, equation (2.8) can then be written as follows:

$$H=T_e+U_{e-e}+V_{e-nuc} \quad \text{.....(2.9)}$$

The first part of equation (2.9) presents the kinetic energy of all electrons, which is described by;

$$T_e=\sum -\frac{\hbar 2}{2m_e}\nabla^2 \quad \text{..... (2.10)}$$

The electron-electron interaction is represented in the second part of equation (2.9), which is given by;

$$U_{e-e} = \sum_{n,m,n\neq m} \frac{e^2}{4\pi\varepsilon_0|r_n-r_m|} \quad \text{..... (2.11)}$$

U_{e-e} describes the sum of all potentials acting on a given electron at position r_n by all other electrons at position r_m .

The third part of equation (2.9) describes the interactions between electrons and nuclei, which is expressed by;

$$V_{e-nuc}=\Sigma_N \Sigma_n \, vnuc(r_n-R_N) \quad \text{..... (2.12)}$$

V_{e-nuc} is the interaction between electrons and nuclei; it depends on the positions of electrons rn and nuclei R_N .

The employment of a Born-Oppenheimer approximation [86], allows the electron and nucleon degrees of freedom to be decoupled.

2-3-1 The Hohenberg-Kohn Theorems

Essentially, density functional theory (DFT) evolved significantly depending on two ingeniously simple theorems put forward and proved by Hohenberg and Kohn in 1964 [87]. These theorems are two powerful statements:

Theorem I: For any system of interacting particles in an external potential V_{ext}, the density is uniquely determined. In other words, the external potential is a unique functional of the density [87].

To prove this theorem, assume that there are two external potentials $V_{ext}^{(1)}$ and $V^{(2)}{}_{ext}$differing by more than a constant, and giving rise to the same ground state density, $\rho_0\,(r)$. It is clear that these potentials belong to different Hamiltonians, which are denoted $H^{(1)}$ and $H^{(2)}$, and they give rise to distinct ground-state wavefunctions $\Psi^{(1)}$ and $\Psi^{(2)}$. Since $\Psi^{(2)}$ is not a ground state of $H^{(1)}$, so:

$$E^{(1)}=\langle\Psi^{(1)}|H^{(1)}|\Psi^{(1)}\rangle<\langle\Psi^{(2)}|H^{(1)}|\Psi^{(2)}\rangle \quad \text{.....(2.13)}$$

and, similarly:

$$E^{(2)}=\langle\Psi^{(2)}|H^{(2)}|\Psi^{(2)}\rangle<\langle\Psi^{(1)}|H^{(2)}|\Psi^{(1)}\rangle \quad \text{..... (2.14)}$$

Assuming that the ground states are non-degenerate [88, 89], one could rewrite equation (2.13) as follows:

$$\langle\Psi^{(2)}|H^{(1)|}\Psi^{(2)}\rangle=\langle\Psi^{(2)}|H^{(2)}|\Psi^{(2)}\rangle+\langle\Psi^{(2)}|H^{(1)}-H^{(2)}|\Psi^{(2)}\rangle=E^{(2)}+\int dr(Vext^{(1)}(r)-Vext^{(2)}(r))\rho_0(r) \quad \text{..... (2.15)}$$

and assuming that $|\Psi^{(1)}\rangle$ has the same density $\rho_0(r)$ as $|\Psi^{(2)}\rangle$:

$\langle\Psi^{(1)}|H^{(2)}|\Psi^{(1)}\rangle=E^{(1)}+\int dr(V^{(2)}{}_{ext}\,(r)-V^{(1)}{}_{ext}\,(r))\rho_0(r)$ ……(2.16)

Combining of equations (2.15) and (2.16) leads to,

$E_{(1)}+E_{(2)}<E_{(1)}+E_{(2)}$ ……(2-17)

This equation proves the two different external potentials cannot produce the same ground-state density.

Theorem II: A universal functional $F[\rho]$ for the energy $E[\rho]$ could be defined in terms of the density. The exact ground state is the global minimum value of this functional. In other words, the ground state energy of the system is given by the functional $F[\rho]$. If the input density and ground-state density are the same, the functional $F[\rho]$ would deliver the lowest energy. Hence, the functional could be minimized by varying the density to obtain the ground-state energy for the external potential.

The second theorem could be proven by considering the expression for the total energy, E, of the system with density ρ.

$E[\rho]=T[\rho]+E_{int[\rho]}+\int drV_{ext(r)}\rho_{(r)}$ …… (2.18)

The kinetic term, T, and internal interaction of the electrons, E_{int}, depend only on the charge density, and so are universal.

The first theorem reported that the ground-state density ρ_0 for a system with external potential V_{ext} and wave function Ψ_0, determines the Hamiltonian of that system, so for any density, ρ, and wave function, Ψ, other than the ground state, it could be found

$E_0=\langle\Psi_0|H|\Psi_0\rangle<\langle\Psi|H|\Psi\rangle=E$ …… (2.19)

Hence, the ground-state density, ρ_0, minimizes the functional (equation 2.18). If the functional $T[\rho]+E_{int}[\rho]$ is known, then by minimizing equation 2.19, the ground-state of the system could be obtained, and then all ground-state characteristics could be calculated, which are the subject of the interest.

2-3-2 Kohn-Sham Method and Self-Consistent Field

Kohn and Sham noticed that Hohenberg-Kohn theory is applicable to both interacting and non-interacting systems. As DFT avoids the interacting many particle problem. The non-interacting system has one great advantage over the interacting system as finding the ground-state energy for a non-interacting system is easier. In 1965, Kohn and Sham came up with the idea, that it is possible to replace the original Hamiltonian of the system by an effective Hamiltonian (H_{eff}) of the non-interacting system in an effective external potential $V_{eff}(\vec{r})$ which gives rise to the same ground state density as the original system. Since there is no clear recipe for calculating this, the Kohn-Sham method is considered as an ansatz, but it is considerably easier to solve than the non-interacting problem. The Kohn-Sham method is based on the Hohenberg-Kohn universal density [81, 85, 90,91]:

$$F_{H-K}[n(\vec{r})] = T_{int}[n(\vec{r})] + U_{ee}[n(\vec{r})] \quad \text{.....(2.20)}$$

The Hohenberg-Kohn functional for non-interacting electrons is reduced to only the kinetic energy. The energy functional of the Kohn-Sham ansatz $F_{K-S}[n(\vec{r})]$, in contrast to (2.18), is given by:

$$F_{K-S}[n(\vec{r})] = T_{non}[n(\vec{r})] + E_{Hart}[n(\vec{r})] + \int V_{ext}(\vec{r})\ n(\vec{r})\ d\vec{r}$$

$$+E_{xc}[n(\vec{r})] \quad \text{.....(2.21)}$$

where T_{non} is the kinetic energy of the non-interacting system which is different than T_{int} (for interaction system) in equation (2.18), while E_{Hart} is the classical electrostatic energy or classical self-interaction energy of the electron gas which is associated with density $n(\vec{r})$. The fourth term E_{xc} is the exchange-correlation energy functional and given by:

$$E_{xc}[n(\vec{r})] = F_{H-K}[n(\vec{r}) - \overbrace{\frac{1}{2}\int \frac{n(\vec{r}_1)n(\vec{r}_2)}{|\vec{r}_1 - \vec{r}_2|} d\vec{r}_1 d\vec{r}_2}^{E_{Hart}[n(\vec{r})]} - T_{non}[n(\vec{r})] \quad \text{……(2.22)}$$

The first, second and third terms in the equation (2.21) can be trivially cast into functional form. In contrast, there is, in general, no exact functional form for E_{xc}. In the last couple of decades, enormous efforts have gone into finding a better approximation toE_{xc}. Currently, the functionals can investigate and predict the physical properties of a wide range of solid state systems and molecules. For the last three terms in the equation (2.21), the functional derivatives can be taken to construct the effective single particle potential $V_{eff}(\vec{r})$[92]:

$$V_{eff}(\vec{r}) = V_{ext}(\vec{r}) + \frac{\partial E_{Hart}[n(\vec{r})]}{\partial n(\vec{r})} + \frac{\partial E_{xc}[n(\vec{r})]}{\partial n(\vec{r})} \quad \text{…… (2.23)}$$

Now, this potential can be used to give the Hamiltonian of the single particle:

$$H_{K-S} = T_{non} + V_{eff} \quad \text{…… (2.24)}$$

By using this Hamiltonian, the Schrödinger equation becomes:

$$[T_{non} + V_{eff}]\Psi_{K-S} = E\Psi_{K-S} \quad \text{…….. (2.25)}$$

Equation (2.25) is known as Kohn-Sham equation. The ground state density $n_{GS}^{K-S}(\vec{r})$ corresponds to the ground state wavefunction Ψ_{GS}^{K-S} which by definition minimizes the Kohn-Sham functional subject to the orthonormalization constraints $\langle\Psi_i|\Psi_j\rangle = \delta_{ij}$; it is found by a self-consistent calculation [78,92,93,94].

Density functional theory uses a self-consistent field procedure. For example, suppose that E_{Hart} and E_{xc} can be accurately determined. The problem is now that V_{eff} cannot be calculated until the correct ground state density is known and the correct density cannot be obtained from the Kohn-Sham wavefunctions until equation (2.25) is solved with the correct V_{eff}. Therefore this circular problem can be solved by carrying out a self-consistent cycle [80,97,98] as shown in Figure 2.1.

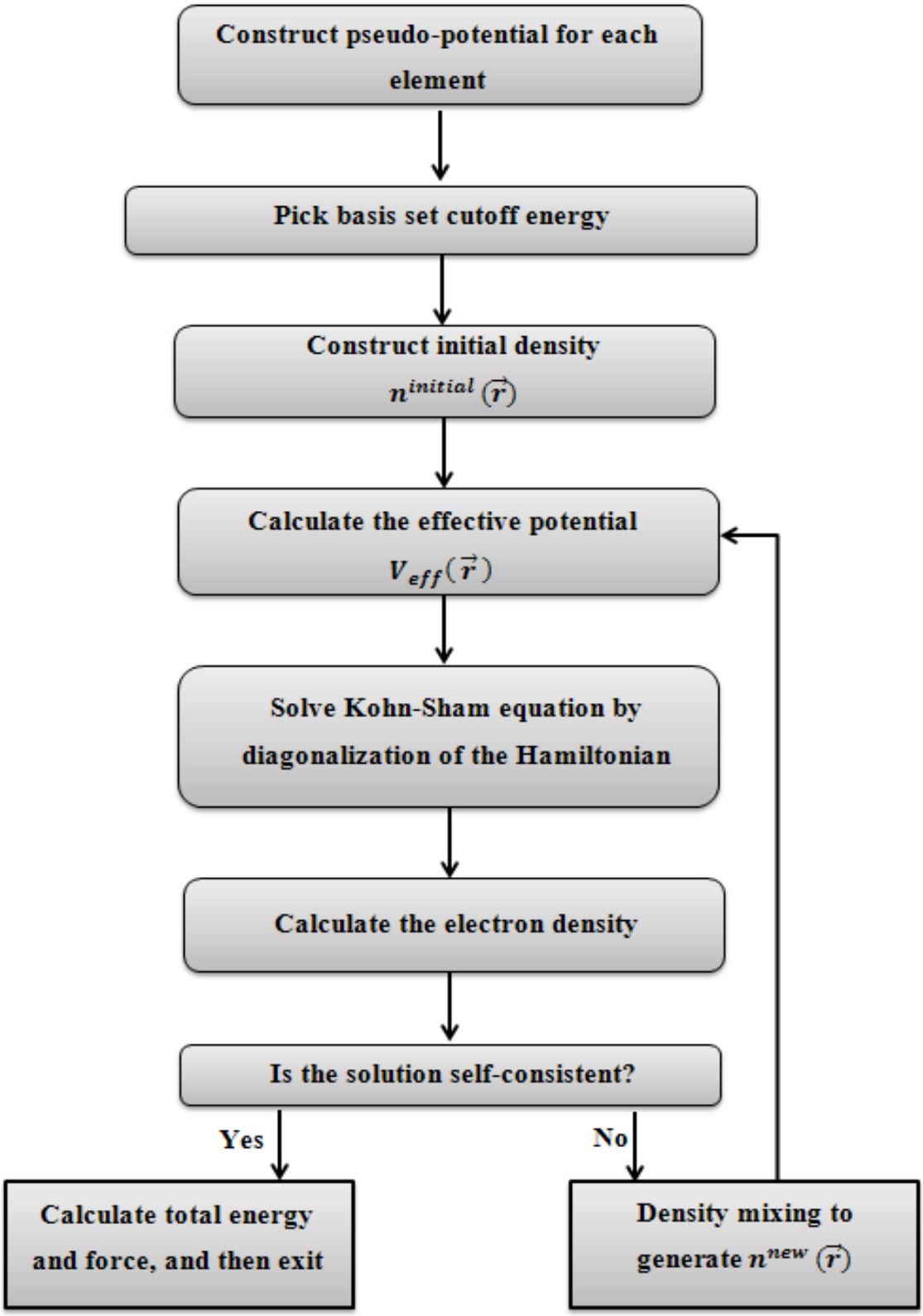

Figure 2-1 A Schematic illustration of the self-consistent DFT cycle [95].

According to Figure 2-1, the first step is to generate the pseudo-potential which represents the electrostatic interaction between the valence

electrons and the nuclei and core electrons. The next step is to build the required basis set with a selected kinetic energy cutoff to be inserted in the basis set; this step is to expand the density functional quantities. Clearly, if the density is known, the energy functional is fully determined. A trial electronic density $n^{initial}(\vec{r})$ is made as an initial guess. This initial guess is used to calculate the following quantity:

$$G = E_{Hart}[n^{initial}(\vec{r})] + E_{xc}[n^{initial}(\vec{r})] \quad \text{……..(2.26)}$$

Then $\frac{\partial G}{\partial n^{initial}(\vec{r})}$ and the effective potential V_{eff} are calculated. The effective potential is used to solve the Kohn-Sham equation (2.25) which leads to finding the electron Hamiltonian. After obtaining the Hamiltonian, it is diagonalised in order to find the eigenfunctions and the new electron density $n^{new}(\vec{r})$. Hopefully, this $n^{new}(\vec{r})$ will be closer to true ground state and is checked. For self-consistency, if this new updated electron density $n^{new}(\vec{r})$ agrees numerically with the density $n^{initial}(\vec{r})$ used to build the Hamiltonian at the beginning of the SCF cycle, we have reached the end of the loop. We then exit, and calculate all the desired converged quantities, such as the total energy, the electronic band structure, density of states, *etc*... Otherwise, the new density $n^{new}(\vec{r})$ does not agree with the starting density $n^{initial}(\vec{r})$, one generates a new input density and starts another SCF cycle: build the new density-dependent Hamiltonian, solve and compute the density, and check for self-consistency [80,84,97].

The Kohn-Sham approach clearly shows that a complicated Many body system can be mapped onto a set of simple non-interacting equations exactly if the exchange correlation functional is known. However, the exchange-correlation functional is not known exactly so approximations need to be made.

2-4 Schrodinger equation

The Schrödinger equation can be used to describe any system composed of several non-relativistic particles:

$$H\Psi_i(\vec{r}_1,\vec{r}_2..\vec{r}_N,\vec{R}_1,\vec{R}_2..\vec{R}_M) = E_i\Psi_i(\vec{r}_1,\vec{r}_2..\vec{r}_N,\vec{R}_1,\vec{R}_2..\vec{R}_M) \quad \text{.....(2.27)}$$

Here, $\widehat{H}$ is the Hamiltonian operator for a system composed of N electrons and M nuclei that describes the interaction of particles, where Ψi denotes the wave function of the system's i^{th} state and E_i denotes the numerical value of the energy associated with the state denoted by Ψi. The Hamiltonian factor for such a system can be expressed as the sum of five terms defined in [98,99].

$$H = \overbrace{-\frac{\hbar^2}{2m_e}\sum_{i=1}^{N}\nabla_i^2}^{T_e} \overbrace{-\frac{\hbar^2}{2m_n}\sum_{n=1}^{M}\nabla_n^2}^{T_n} \overbrace{-\frac{1}{4\pi\varepsilon_o}\sum_{i=1}^{N}\sum_{n=1}^{M}\frac{Ze^2}{|\vec{r}_i-\vec{R}_n|}}^{U_{en}} + \overbrace{\frac{1}{8\pi\varepsilon_o}\sum_{i=1}^{N}\sum_{j\neq i}^{N}\frac{e^2}{|\vec{r}_i-\vec{r}_j|}}^{U_{ee}}$$
$$+ \overbrace{\frac{1}{8\pi\varepsilon_o}\sum_{n=1}^{M}\sum_{n\neq\acute{n}}^{M}\frac{Z_nZ_{\acute{n}}e^2}{|\vec{R}_n-\vec{R}_{\acute{n}}|}}^{U_{nn}}$$

……..(2.28)

Here i and j denote the N-electrons while n and n' running on the M-nuclei in the system, m_e and m_n are the mass of the electron and nucleus respectively, e and Z_n are the electron and nuclear charge respectively. The position of the electrons and nuclei are denoted as $\vec{r}_i$ *and* $\vec{R}_n$ respectively.

In the equation (2.28), the first and second terms, T_e and T_n represent the kinetic energy of electrons and nucleus, respectively. The last three terms represent the potential part of the Hamiltonian; where U_{en} defines the attractive electrostatic interaction between electrons and nucleus. Electron-

electron, U_{ee} and nuclear-nuclear, U_{nn} describe the repulsive part of the potential respectively [98,99].

When solving the Schrödinger equation (Equation 2.27) and knowing the wave function Ψ, all important physical quantities can be calculated. However, even for modest system sizes - even for a few atoms - the general problem is virtually impossible even on modern supercomputers [99].

The virtue of density functional theory is that it expresses the physical quantities in terms of the ground-state density. The electronic density of a general many body state, characterized by a wave function $\Psi(r_1,r_2\ldots..r_{n)}$, is defined as [100]:

$$\rho(r) = \int dr_1\, dr_2 dr_3 \ldots\ldots\ldots dr_i\, |\Psi(r_1, r_2, r_3 \ldots\ldots r_i|^2 \qquad \ldots\ldots\ldots(2.29)$$

2-5 Time-Dependent Density Functional Theory (TD-DFT)

The time-dependent density functional theory (TD-DFT) extends the ground-state density functional theory by allowing for the examination of a system's excited-state features in the presence of time-dependent potentials, such as electric or magnetic fields. TD-DFT may be used to investigate the influence of fields on molecules by calculating representative excitation energies, oscillator strength, wavelength, molecular orbital character, and electronic transitions of the molecules [101].

The theoretical of TD-DFT based on the Runge-Gross theorem (R-G theorem) in 1984. The R-G theorem explained the association between the time-dependent external potential $\hat{V}_{ext}(\vec{r})$ and $\rho(\vec{r}\,,t)$ of the system. R-G theorem designated that when two external potentials $\hat{V}_{ext}(\vec{r})$ and $\widehat{V'}_{ext}(\vec{r})$ have an alteration of more than a time-dependent function, their own electron densities $\rho(\vec{r}\,,t)$ and $\rho'(\vec{r}\,,t)$ are also dissimilar [102].

Runge and Gross discussed how excited states are obtained using TD-DFT. The starting point of studying time-dependent systems is the time-dependent Schrodinger equation. The TD-DFT is straight related to the Schrodinger equation $\left[\boldsymbol{i}\,\hbar\,\frac{\boldsymbol{\partial}}{\boldsymbol{\partial t}}\,\boldsymbol{\Psi}\,(\,\vec{\boldsymbol{r}}\,,\boldsymbol{t}\,) = \hat{\boldsymbol{H}}\,\boldsymbol{\Psi}\,(\,\vec{\boldsymbol{r}}\,,\boldsymbol{t}\,) \right]$ where the Hamiltonian is known to be [103]:

$$\hat{H} = \hat{T} + \hat{V}_{\text{elec.elec}} + \hat{V}_{\text{ext.}}(\vec{r}\,) \qquad \text{……..(2.30)}$$

Here, $\hat{H}$ consists of the kinetic energy operator $\hat{T}$ electron-electron repulsion $\hat{V}_{\text{elec.elec}}$ (Coulomb operator) and the external potential $\hat{V}_{\text{ext.}}(\vec{r})$. Where $\hat{V}_{\text{ext.}}(\vec{r})$ is given in the following operators:

$$\hat{V}_{\text{ext.}}(\vec{r}) = \sum_{i=1}^{N} \hat{V}\text{ext.}(\vec{r_i}\,) \qquad \text{……(2.31)}$$

The densities of the system rise from a fixed first state $\Psi\,(\,t_o) = \Psi\,(\,0\,)$. The first state, $\Psi\,(\,0)$ is arbitrary, it must not be the ground-state or some other eigen state of the first potential $\hat{V}\text{ext.}(\vec{r}) = \hat{V_o}\,(\vec{r})$. The R-G theorem indicates that there exists an one-to-one correspondence between the time-dependent external potential $\hat{V}\text{ext.}(\vec{r})$, and the time-dependent electron density $\rho(\vec{r}\,,t)$, for systems developing from a fixed first many-body state. Translation to it, the density determines the external potential, and next helps in obtaining the time-dependent many-body wave functions [104].

As this wave-function controls all observables of the system as an important, the saying point is that all observables are functionals of $\rho(\vec{r}\,,t)$. The statement of the theorem is the "densities $\rho(\vec{r}\,,t)$ and $\rho'(\vec{r}\,,t)$ evolving from the same initial state $\Psi(0)$ under the effect of two potentials $\hat{V}\text{ext.}(\vec{r})$ and $\widehat{V'}_{ext}(\vec{r})$ are always different provided that the

potentials differ by additional than a chastely time-dependent function [101,103]:

$$\hat{V}\text{ext.}(\vec{r}\,,t) = \widehat{V}_{ext}(\vec{r}\,,t) + C(t) \quad \text{……. (2.32)}$$

Where the C(t) allows increase to wave functions that are different only by a phase factor $e^{-iC(t)}$, therefore, the same electronic density is stable. R-G theorem states that the density is a functional of the external potential and of the first wave function on the space of potentials differing by more than the addition of C(t).

2-6 SIESTA

The DFT electronic structure calculations have been performed using the SIESTA code[4]. One of the main features of SIESTA is that it is designed to perform efficient calculations on huge systems consisting of thousands of atoms, and it uses the standard Kohn-Sham self-consistent density function method. In addition, the functionals that are used in SIESTA are the Local Density Approximation (LDA) and the Generalized

Gradient Approximation (GGA). In this section, we will explain briefly the important methods and how they are used to perform all DFT calculations.

2-6-1 The Pseudopotential Approximation

In a system that has a large number of atoms containing complex potentials there is large computational expense for time and memory. One method to solve the computational problem is to reduce the number of electrons by introducing the pseudopotential approximation which was proposed by Fermi in 1934 [105-106].

This method, has developed from creating non-relativistic empirical pseudopotentials [107,108] to more realistic ab-initio pseudopotentials [109-110].

The idea of this concept that the electrons in an atom are split into two parts, the first is core and the second is valence, where core electrons lie within filled atomic shells as well as they are spatially localized around the nucleus. Whereas, the valence electrons are arranged in partially filled shells, and they are the ones contributing to the formation of molecular orbitals.

Therefore, this reduces the number of the electrons in a system considerably. Moreover, in the SIESTA code a special kind of ab-initio pseudopotential which called the norm-conserving pseudopotential [109] is carried out. There are many advantages of using pseudo-potentials in the computational calculations which are:

1- To reduce the number of the electrons which are participating in the calculations by removing the core electrons from the calculations which leads to decrease both time and memory required to run the ab-initio simulation.
2- The total energy scale is greatly reduced when the core electrons are removed from the calculation and that makes the numerical calculation of energy differences between atomic configurations much more stable.
3- By introducing pseudo-potentials and replacing the true valence wavefunctions by pseudo-wavefunctions, to exactly match the true valence wavefunctions outside of the core or cutoff radius $\boldsymbol{r_c}$, but are nodeless inside. These pseudo-wavefunctions can be expanded using a much smaller number of the plane wave basis states.

4- A further advantage of using pseudo-potentials is that relativistic effects can be added easily into the pseudo-potential whilst further treating the valence electrons non–relativistically.

2-6-2 Localised Atomic Orbital Basis Sets (LAOBs)

One of the most important aspects of the SIESTA code is the type of the basis function employed in the calculations. It uses a basis set composed of localised atomic orbitals which compare well with other DFT schemes which may use a plane wavefunction basis set [111]. The benefits from using LAOBs are that they provide a closer representation of the chemical bond; they can allow order-N calculations to be performed and also it gives a good base from which generate a tight-binding Hamiltonian. SIESTA uses confined orbitals, i.e. orbitals are constrained to be zero outside of a certain radius (cutoff radius r_c). This produces the desired sparse form of the Hamiltonian as the overlap between basis functions is reduced. The atomic orbitals inside this radius are products of a numerical radial function and a spherical harmonic. The simplest form of the atomic basis set for an atom (labelled as I) is called single-ζ (also called minimal) which represents a single basis function per electron orbital. It is given by the following equation [112]:

$$\Psi^{\mathrm{I}}_{nlm}(\vec{r}) = R^{\mathrm{I}}_{nl}(\vec{r})\, Y^{\mathrm{I}}_{lm}(\vec{r}) \qquad \text{.....(2.33)}$$

where $\Psi^{\mathrm{I}}_{nlm}(\vec{r})$ is the single basis function which consists of two parts, the first part is the radial wavefunction R^{I}_{nl} and the second part is the spherical harmonic Y^{I}_{lm}. Minimal or single zeta basis set are constructed by using one basis function of each type occupied in the separate atoms that comprise a molecule. If at least one ***p-type*** orbital is occupied in the atom, then the complete set (*3p-type*) of the functions must be included in the

basis set. For example, in the carbon atom, the electron configuration is $1s^2\ 2s^2\ 2p^2$, therefore, a minimal basis set for carbon atom consists of $1s, 2s, 2p_x, 2p_y$ and $2p_z$ orbitals which means the total basis functions are five as shown in Table 2-1 [111].

Higher accuracy basis sets called multiple-ζ are formed by adding another radial wavefunctions for each included electron orbital. Double basis sets are constructed by using two basis functions of each type for each atom.

For carbon atom, a double zeta basis contains ten basis function corresponding to ten orbitals which are $1s, \mathbf{1s'}, \mathbf{2s}, \mathbf{2s'}, \mathbf{2p_x}, \mathbf{2p'_x}, \mathbf{2p_y}, \mathbf{2p'_y}, \mathbf{2p_z}$ **and** $\mathbf{2p'_z}$. For further accuracy, polarisation effects are included in double-ζ polarised basis sets obtained by including wavefunctions with different angular momenta corresponding to orbitals which are unoccupied in the atom.

A polarization function is any higher angular momentum orbital used in a basis set which is unoccupied in the separated atom. As an example, the hydrogen atom has only one occupied orbital type that is *s*-type. Therefore, if *p*-type or *d*-type basis functions were added to the hydrogen atom they would be known as polarization functions. Carbon atoms with polarization functions include *d*-type and *f*-type basis functions.

Table (2-1): Examples of the radial basis sets functions per atom used in SIESTA code for different precisions of the split valence basis sets [111].

Atom/Basis Functions	Single-ζ (SZ)	Double-ζ (DZ)	Single-ζ Polarised (SZP)	Double-ζ Polarised (DZP)
$H^1/1s$	1	2	4	5
$C^6/1s\ 2s\ 2p_x 2p_y 2p_z$	4	8	9	13
$N^7/1s\ 2s 2p_x 2p_y 2p_z$	4	8	9	13

Assuming the core electrons (non-valence electrons) of an atom are less affected by the chemical environment than the valence electrons. This is so-called as split valence basis set. For example, the carbon atom, a split valence double zeta basis set would consist of a single $1s$ orbital, along with $2s, 2s'$and $2p_x, 2p'_x, 2p_y, 2p'_y, 2p_z, 2p'_z$ orbitals, for a total of 9 basis functions. The basis functions in a split valence double zeta basis set are denoted $1s, 2s, 2s', 2p_x, 2p'_x, 2p_y, 2p'_y, 2p_z, 2p'_z$. In case of molecules, molecular orbitals can be represented as Linear Combinations of Atomic Orbitals (LCAO-MO) given by [112,113]:

$$\varphi_i(\vec{r}) = \sum_{\upsilon=1}^{L} a_{\upsilon i}\ \Psi_\upsilon(\vec{r}) \qquad \text{……(2.34)}$$

where φ_i represents the molecular orbitals (basis functions), Ψ_υ are atomic orbitals, $a_{\upsilon i}$ are numerical coefficients and L is the total number of the atomic orbitals.

2-6-3 SIESTA Basis Sets

It is self-evident that the Hamiltonian must be diagonalised in order to find the wave functions. This operation entails the inversion of a large matrix, the computing time of which scales according to the number of non-zero members. As a result, for efficient calculations, the Hamiltonian must be sparse with a large number of zeros. SIESTA makes use of a Linear Combination of Atomic Orbitals (LCAO) basis set, which is formed from the atoms' orbitals and is required to be zero after a predetermined cut-off radius. As the overlap between basis functions decreases, the former produces the needed sparse form of the Hamiltonian, while the latter permits even a small basis set to yield properties similar to those of the examined system. The simplest basis set for an atom is called a single ζ basis, which corresponds to a single basis function, $\Psi_{nlm}(r)$ per electron orbital (i.e. 1 for an s-orbital, 3 for a p-orbital, etc.). In this case each basis function consists of a product of one radial wave function, $\emptyset_{nl}^{1}$ and one spherical harmonic Y_{lm}:

$$\Psi_{nlm}(r) = \emptyset_{nl}^{1}(r)\, Y_{lm}(\theta, \emptyset) \qquad \text{…….(2.35)}$$

The radial part of the wave function is found by using the method proposed by Sankey [113,114], where the Schrodinger equation is solved for the atom placed inside a spherical box. It is under the constraint to vanish at a cut-off radius r_c. This constraint produces an energy shift δE within the Schrödinger equation such that the eigen functions first node occurs at r_c:

$$\left[-\frac{d^2}{dr^2} + \frac{l(l+1)}{2r^2} + V_{nl}^{ion}(r)\right]\emptyset_{nl}^{1}(r) = (\varepsilon_{nl} + \delta E)\emptyset_{nl}^{1}(r) \qquad \text{……..(2.36)}$$

For higher accuracy basis sets (multiple-ζ), additional radial wave functions can be included for each electron orbital. The additional radial wave functions, phi_{nl}^{i} for $i > 1$, are calculated using a split-valence method. This involves defining a split valence cut off for each additional wave function r_s^i , so it is split into two piecewise functions: a polynomial below the cut-off and the previous basis wavefunction above it:

$$\emptyset_{nl}^{i}(r) = \begin{cases} r^l(a_{nl} - b_{nl}r^2) & r < r_s^i \\ \emptyset_{nl}^{i-1} & r_s^i < r < r_s^{i-1} \end{cases} \qquad \text{……..(2.37)}$$

The additional parameters are found at the point r_s^i where the wavefunction and its derivative are assumed continuous.

Further accuracy (multiple-ζ polarized) can be obtained by including wave functions with different angular momenta corresponding to orbitals which are unoccupied in the atom. This is done by solving (Eq. 2.37) in an electric field such that the orbital is polarized or deformed due to the field (see [115] for details) so a different radial function is obtained. This is now combined with the appropriate angular dependent spherical harmonic which increases the size of the basis. Table (2.1) shows the number of basis orbitals for a selected number of atoms for single-ζ, single- ζ polarized, double- ζ and double- ζ polarized.

Table (2-2): Examples of the radial basis functions per atom as used within the SIESTA for different degrees of precisions[69].

Basis Set	**H**	**C**	**Au**
Single-ζ (SZ)	1= (1 × 1s)	4= (1×2s+3×2p)	6 = (1 × 6s + 5 × 5d)
Double-ζ (DZ)	2= (2 × 1s)	8 = (2×2s +6×2p)	12 = (2 × 6s + 10 × 5d)
Single-ζ Polarised (SZP)	4=(1×1s+3×2p)	9 = (1×2s+3×2p+5×3$\tilde{d}$)	9 = (1× 6s+5×5d+3×6$\tilde{p}$)
Double-ζ Polarised (DZP)	5=(2×1s+3×2p)	13 = (2×2s+6×2p+5×3$\tilde{d}$)	15 = (2×6s+10×5d+3×6$\tilde{p}$)

2-6-4 Structure Optimisation

In this thesis, the SIESTA code is used to obtain the ground state energy of different atomic configurations, and then obtain the relaxed structure of the systems. This means that SIESTA can provide us the energy as a function of the atomic coordinates (position of atoms). The structure optimisation (also known as geometry optimisation) contains three options; relaxing atomic coordinates, allowing periodic cell shapes and volumes to change.

In case of full optimisation, the three options can be employed together, which leads to the minimum energy of the atoms in the system and the equilibrium lattice parameters of the systems. Performing the relaxation of the atomic positions allows atoms to move until the residual force between all atoms is smaller than the required convergence tolerance in eV/Å.

In structural optimisation the force is the key quantity and this force could be calculated numerically by taking the approximate numerical derivatives of the total energy with respect to the positions. This method is applied in SIESTA using the Hellmann-Feynman theorem [116].

2-7 The Exchange Correlation Functional

There are numerous proposed forms for the exchange and correlation energy in the literature. The first successful - and yet simple - form was the Local Density Approximation (LDA) [117, 118], which depends only on the density and is therefore a local functional.

Then the next step was the Generalized Gradient Approximation (GGA) [119-120], including the derivative of the density it also contains information about the neighborhood and therefore is semi-local.

LDA and GGA are the two most commonly used approximations to the exchange and correlation energies in density functional theory.

There are also several other functionals, which go beyond LDA and GGA. Some of these functionals are tailored to fit specific needs of basis sets used in solving the Kohn-Sham equations (Eq. 2-25) and a large category are the so called hybrid functionals (eg. B3LYP, HSE [121] and Meta hybrid GGA [122, 123]), which combine the LDA and GGA forms.

One of the latest and most universal functionals, the Van der Waals density functional (vdW-DF) [124], contains non-local terms and has proven to be very accurate in systems where dispersion forces are important [125,126].

The following sections will briefly describe the Local Density Approximation and the Generalized Gradient Approximation.

2-7-1 Local Density Approximation (LDA)

Based on Kohn-Sham method, the functional E_{xc} functional could be calculated in a homogenous electron gas to approximate the many body particle problem as a simpler system [84]. Kohn-Sham demonstrated that by slowly varying the density of a system, the E_{xc} functional at point $\vec{r}$ can be considered as acting in a uniform density. Therefore the E_{xc} functional can be represented by a uniform electron gas $E_{xc}^{homo}[n(\vec{r})]$ with a density $n(\vec{r})$.

In general the LDA will not work for systems which are dominated by electron-electron interactions. However, LDA supposes that the density is a constant in the local region around any considered position and it is given by [81,95]:

$$E_{xc}^{LDA}[n(\vec{r})] = \int E_{xc}^{homo}[n(\vec{r})]n(\vec{r})d\vec{r}\,. \qquad \text{…..(2.38)}$$

The exchange-correlation energy $E_{xc}^{homo}[n(\vec{r})]$ can be split into two terms as the sum of the exchange $E_{x}^{homo}[n(\vec{r})]$ and the correlation energies $E_{c}^{homo}[n(\vec{r})]$ which can be found separately as:

$$E_{xc}^{homo}[n(\vec{r})] = E_{x}^{homo}[n(\vec{r})] + E_{c}^{homo}[n(\vec{r})] \qquad \text{……(2.39)}$$

The exchange term can be found analytically; it is well known and can be found in many textbooks [81-95]. and it is given by:

$$E_x^{homo}[n(\vec{r})] = -\frac{3}{4}\left(\frac{3n(\vec{r})}{\pi}\right)^{1/3} \quad \text{……. (2.40)}$$

The correlation energy ($E_c^{homo}[n(\vec{r})]$) term cannot be obtained analytically, but it can be calculated accurately using numerical methods. The most common and accurate method was proposed by **C**eperly and **A**lder **(CA)** [127] using quantum Monte-Carlo simulations. There are several different interpretations of the Monte Carlo data, for example, the most used was calculated by **P**erdew and **Z**unger (PZ), who fitted this numerical data to an analytical expression and obtained [128,129]:

$$\boldsymbol{E_c^{homo}[n(\vec{r})]} = \begin{cases} -0.048 + 0.031\, ln(r_o) - 0.0116\, r_o + 0.002\ ln(r_o)\ \ if\ r_o < 1 \\ -\dfrac{0.1423}{(1 + 1.9529\sqrt{r_o} + 0.3334\, r_o}\ if\ r_o > 1 \end{cases} \quad \text{…..(2.41)}$$

here r_o is the average radius of the electrons in the homogenous electron gas and defined as $\left(\frac{3}{4\pi n}\right)^{1/3}$.

The LDA is a simple and well known powerful functional, it is considered to be accurate for graphene and carbon nanotubes or where the electron density is not rapidly changing. A larger error is expected for atoms with *d* and *f* orbitals. This functional to some extent has many pitfalls, for example the band gap in semiconductors and insulators is usually not accurate with a large error (in the range of 0.5 to 2eV or 10-30%). For this reason it is highly advisable to seek better functionals [128,130,131].

2-7-2 Generalized Gradient Approximation

GGA extends LDA by including the derivatives of the density into the functional form of the exchange and correlation energies. In this case there exists no closed form for the exchange part of the functional, hence it has to be calculated along with the correlation contributions using numerical methods. Just as in the case of the LDA there exist many parameterizations for the exchange and correlation energies in GGA [132-133].

LDA and GGA are the two most commonly used approximations for the approximation of exchange-correlation energies in the DFT. Also, there are several other functionals, which go beyond LDA and GGA. In general, there is no robust theory of the validity of these functionals. It is determined via testing the functional for various materials over a wide range of systems and comparing results with reliable experimental data.

2-7-3 The Hybrid Functional

The hybrid functionals are extremely good at accurately representing a wide variety of molecular characteristics. Calculating the exact (Hartree-Fock) exchange in big molecules and solids, particularly in systems with metallic properties, is computationally expensive. The most widely used hybrid functional, B_3LYP, employs Becke's 1988 exchange function (E_X^{B88}) and Lee Yang and Parr's correlation function (E_C^{LYP}) as gradient adjustments to the LSDA exchange and correlation functions, respectively [135-101].

$$E_{XC}^{B_3LYP} = (1 - a)E_X^{LSDA} + a\,E_X^{HF} + bE_X^{B88} + c\,E_C^{LYP} + (1 - c)E_C^{LSDA} \quad \ldots(2\text{-}42)$$

The three parameters are: a=0.20, b=0.72 and c=0.81. Where'a' specifies the amount of exact exchange, and 'b' and 'c' control the contribution of exchange and correlation, respectively.

2-8 Theory of Quantum Transport

The purpose of molecular electronics is to gain an understanding of the electrical properties and behavior of molecular junctions. One of the difficulties is delivering molecular structures of electrode blocks for the purpose of examining their electrical properties. Connection In general, the force between the molecule and the metal electrode has a significant role. In determining the transport properties of a lead | molecule | lead frame as a result of scattering processes within the lead | molecule | lead frame. The primary theoretical way for understanding scattering in this System is using the Green's function formalities [115].

Our objective in this section is to gain a general understanding of Landauer's formalism, and we will begin with a simple derivation of the Landauer formula. A one-dimensional construction is presented to demonstrate the overall methods utilized in the description. Transport in arbitrarily complex-geometry intermediate conductors. Assume this procedure. The interaction between carriers and inelastic processes is negligible, which is a well-known fact for molecules less than 3nm in length at ambient temperature [103].

2-8-1 Green's Function Scattering Formalism

We apply a Green function scattering formalism to determine the transmission coefficient of a molecule coupled to semi-infinite leads. This is a continuation of the next chapter's discussion of calculating the electronic structure of an isolated molecule using DFT. The isolated

molecule's properties and the interaction between the molecule and the electrodes have an effect on the open system's electronic properties. As a result, transport models must account for both aspects in order to comprehend the electron scattering process between the two electrodes [114].

To begin, it is necessary to determine the scattering matrix for a basic one-dimensional system. This section will detail the approach employed. Due to the fact that Green's function will be employed in the derivation.

2-8-1-1 Perfect One-Dimensional Lattice

In this section will discuss what the Green's function looks like for a simple one dimensional lattice with on-site energies ε_o and real hopping parameters as shown in Figure (2-2 **).**

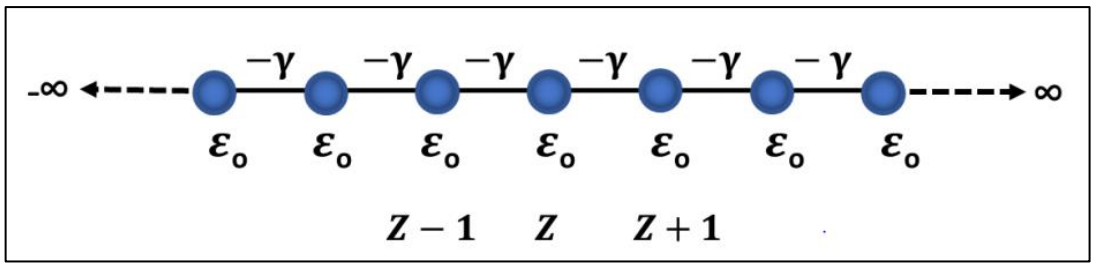

Figure (2-2) One-dimensional periodic lattice tight-binding approximation with on-site energies ε_o and hopping parameters γ[114].

The Schrödinger equation describes the wave function of the system with Hamiltonian H[114,115],

$$\hat{H}\,\psi = E\,\psi \qquad \text{..... ...(2.43)}$$

Wave function Ψ_z it is expanded into a one-dimensional orthogonal localized basis set $|z'\rangle$:

$$|\psi\rangle = \sum \psi_{z'} |z'\rangle \quad \text{..}\ldots\ldots\ldots\ldots(2.44)$$

Substituting (Eq. 2.44) in (Eq. 2.43) and multiply the result by $|z\rangle$ we get:

$$\sum H_{z,z'} \psi_{z'} = E\psi_z \quad \text{..}\ldots\ldots\ldots\ldots(2.45)$$

Hence,

$$H_{z,z'} = \langle z|\hat{H}|z'\rangle \quad \ldots\ldots\ldots\ldots(2.46)$$

The matrix form of the Hamiltonian can be simply written:

$$H = \begin{pmatrix} \ddots & -\gamma & 0 & 0 \\ -\gamma & \varepsilon_o & -\gamma & 0 \\ 0 & -\gamma & \varepsilon_o & -\gamma \\ 0 & 0 & -\gamma & \ddots \end{pmatrix} \quad \ldots\ldots\ldots\ldots(2.47)$$

the Schrödinger equation (Eq. 2.43) can be expanded at a lattice site z in terms of the energy and wave function ψ_z (Eq. 2.44) [114].

$$(E - H)\psi = 0 \quad \ldots\ldots\ldots..(2.48)$$

$$\varepsilon_o \psi_z - \gamma\psi_{z+1} - \gamma\psi_{z-1} = E\psi_z \quad \text{..}\ldots\ldots\ldots...(2.49)$$

By using the wave function as given by Block's theorem for the perfect lattice chain which has the form $\psi_z = \frac{1}{\sqrt{v_g}}\, e^{ikz}$, where $-\pi \leq k < \pi$. The Schrödinger equation (2.49) can be solved to give the dispersion relation:

$$E = \varepsilon_o - 2\gamma\, cosk \quad \ldots\ldots\ldots\ldots(2.50)$$

Where we introduced the quantum number, k, commonly referred to as the wavenumber[104,114].

To calculate the retarded Green's function $g(z, z')$, which is closely related to the wave function, the following equation is solved:

$$(E - H)g(z, z') = \delta_{z,z'} \quad \text{.....(2.51)}$$

Physically, the lagging Green's function, $g\ (z,\ \acute{z})$, describes the response of a system at point z due to a source at point $\acute{z}$. Intuitively, would expect such excitation to give rise to two waves, which travel outward from the excitation point, with amplitudes A and B as shown in Figure 2- 3[114].

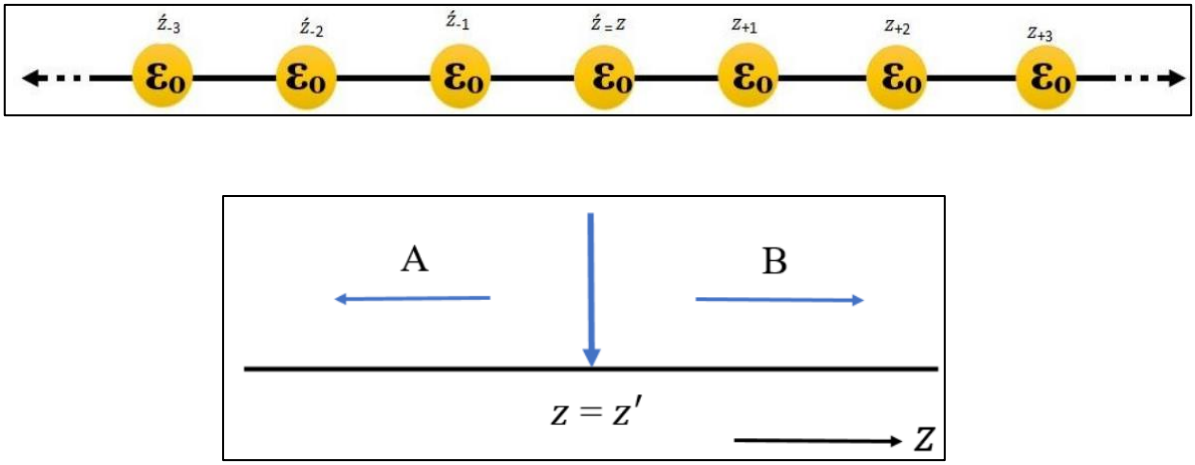

Figure (2-3) Retarded Green's function of an infinite one-dimensional lattice. The excitation at z = z ′ causes waves to propagate left and right with amplitudes A and B respectively[114].

These waves can be expressed simply as:

$$g(z, z') = Be^{ikz}\ z > z'$$

$$g(z, z') = Ae^{-ikz}\ z < z' \quad \text{.....(2.52)}$$

In this equation, the solution satisfies (Eq. 2.51) at every point except $z = z'$. To overcome this, the Green's function must be continuous (Eq. 2.53), so the two are equal at $z = z'$[114]:

$$[g(z,z^{'})]_{z=z^{'}\,left} = [g(z,z^{'})]_{z=z^{'}\,right} \quad \text{.....(2.53)}$$

$$Be^{ikz} = Ae^{-ikz} \implies A = Be^{2ikz} \quad \text{.....(2.54)}$$

By substituting (Eq. 2.61) into the Green's function (Eq. 2.52), we will find as shown:

$$g(z,z') = Be^{ikz} = Be^{ikz'}\, e^{ik(z-z')}\; z > z'$$

$$g(z',z) = Be^{2ikz'}e^{-ikz} = Be^{ikz'}\, e^{ik(z'-z)}\; z < z' \quad \text{.....(2.55)}$$

We can rewrite (Eq. 2.55) as:

$$g(z',z) = Be^{2ikz'}e^{ik|z-z'|} \quad \text{.....(2.56)}$$

To find the value of the constant B, we use equation (2.51) and use Eq. (2.49) which for $z = z'$ given[114].:

$$(\varepsilon_o - E)B - \gamma Be^{ik} - \gamma Be^{ik} = 1 \quad \text{.....(2.57)}$$

$$\gamma B\left(2cosk - 2e^{ik}\right) = 1$$

$$B = \frac{1}{2i\gamma sink} = \frac{1}{i\hbar v_g}$$

where the $\boldsymbol{v_g}$ group velocity, found from the dispersion relation equation (2.51), is:

$$v_g = \frac{1}{\hbar}\frac{\partial E(k)}{\partial k} = \frac{2i\gamma sink}{\hbar} \quad \text{.....(2.58)}$$

We can rewrite the retarded Green's function as shown:

$$g^R(z-z') = \frac{1}{i\hbar v_g}e^{ik|z-z'|} \quad \text{.....(2.59)}$$

The literature [138,139] shows a more extensive derivation. The next step is to submit a file defect in the lattice to create a scattering area and then the transmission coefficient can be calculated.

To Calculate the Green's function for in this problem, we can get the scattering amplitudes. So, form a solution Equation (2.51), which is given as follows:

$$G = (E - H)^{-1} \qquad \text{.....(2.60)}$$

This equation can be singular if the energy E is equal to the Hamiltonian eigenvalues H, to deal with this, it is practical to consider the limit:

$$G_{\mp} = \lim_{\eta \to 0}(E - H \pm i\eta)^{-1} \qquad \text{.....(2.61)}$$

Here η is a positive number and G+, G- is the retarded (advanced) Green's function. The sign of the positive infinitesimal η determines the type of solution which is either a retarded (-) or advanced (+) Green function. Generally, the methodology of computing electron transport is focused on computing a Green function for the infinite system, which includes the leads and the scattering region [136,137].

In the case where there is no coupling between the molecule and the leads, α = 0, the Green's function can be given as:

$$g = \begin{pmatrix} -\frac{e^{ik}}{\gamma} & 0 \\ 0 & -\frac{e^{ik}}{\gamma} \end{pmatrix} = \begin{pmatrix} g_L & 0 \\ 0 & g_R \end{pmatrix} \qquad \text{.....(2.62)}$$

If we consider a switch on of the interaction, then to obtain the Green's function of the coupled leads of this system, G, Dyson's equation is written:

$$G^{-1} = (g^{-1} - V) \qquad \text{……(2.63)}$$

where V is the operator that describes the interaction connecting the leads, which has the form:

$$V = \begin{pmatrix} 0 & V_c \\ V_c^{\dagger} & 0 \end{pmatrix} = \begin{pmatrix} 0 & \alpha \\ \alpha^{*} & 0 \end{pmatrix} \qquad \text{……(2.64)}$$

The solution to Dyson's equation, (Eq. 2.63) reads:

$$G = \frac{1}{|\alpha|^2 - \gamma^2 e^{-2ik}} \begin{pmatrix} \gamma e^{-ik} & \alpha \\ \alpha^{*} & \gamma e^{-ik} \end{pmatrix} \qquad \text{…….(2.65)}$$

The only step left is to calculate the transmission, t, and reflection, r, amplitudes from the Green's function (Eq. 2.65). This is done by taking advantage of the Fisher-Lee relation [116] that relates the scattering amplitudes of a scattering problem to Green's function of the problem. Since $A = B = 1/i\hbar v g$, the equation (2.66) gives a definition for the transmission and reflection coefficients, equations (2.67) and (2.68): The Fisher-Lee relations in this case state that:

$$G_{1,1} = \frac{1}{i\hbar v_g} (1 + r)$$

$$G_{2,1} = \frac{1}{i\hbar v_g} t\, e^{ik} \qquad \text{……..(2.66)}$$

$$r = i\hbar v_g\, G_{1,1} - 1 \qquad \text{……(2.67)}$$

And

$$t = i\hbar v_g \, G_{2,1} e^{ik} \quad \text{.....(2.68)}$$

Therefore, these amplitudes will be corresponded to particles incident from the left. On the other hand, particles are travelling from the right side, which means these expressions could be used for transmission t' and reflection r' amplitudes. According to these coefficients above, the probability can be defined: T = tt*, R = rr*. Consequently Thus, the transmission probability for this case can be given as:

$$T = \frac{\sigma^2}{(\gamma^2 - \alpha^2)^2 + \sigma^2} \quad \text{.....(2.69)}$$

The parameters in this equation are $\sigma = 2\gamma\alpha sink$, and if α = γ that means the transmission T=1. In the case when α is greater or smaller than γ, which leads to create scattering region, and could be resulted to the transmission T ≤ 1.

2.8.2 The Landauer formula

Standard theoretical model to describe the transport phenomenon in ballistic mesoscopic the systems are Landauer's formula [138], a method applicable to phase cohesive systems. First of all, we assume that the system connects two large Scattering tanks, as shown in Fig. 2.4, in this case all are inelastic relaxation processes are limited to tanks [114]. Therefore, the electron is transferred passage through the system is formed as a quantum mechanical scattering problem. The second important assumption is that this system is connected to external tanks by an ideal quantum wire, which acts as a waveguide for electron waves.

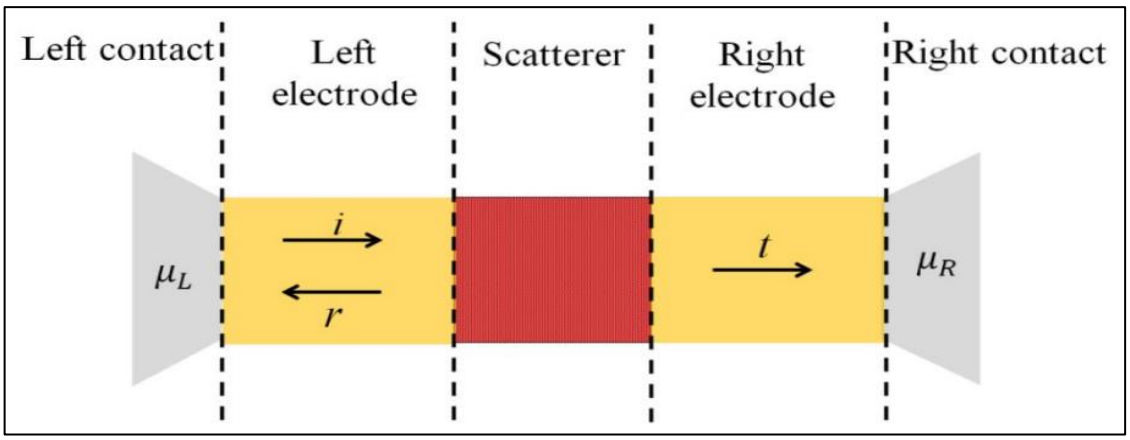

Figure (2-4): Shows a mesoscopic scatterer connected to the contacts by ballistic filaments. The μ_L and μ_R represent the chemical potential at the contacts. When the incident wave packet hits the scatterer on the left, it will be sent with probability $T = tt^*$, it is reflected with probability $R = rr^*$ where, t, t^* , r and r^* represent the transmission and reflection amplitudes from left to the right and vice versa. It requires the conservation of charges T + R = 1[139].

Mesoscopic scattered as shown in Fig.2-4, connected to two electron tanks, and these reservoirs have slightly different chemical potentials $\mu_L - \mu_R = \delta E > 0$, and it causes electrons to move from the left to the right tank. We will discuss the solution to one channel open to one electron: the incident electric current δI which is generated by the chemical potential gradient, as indicated by:

$$\delta I = ev_g \frac{\partial n}{\partial E} \delta E = ev_g \frac{\partial n}{\partial E} (\mu_L - \mu_R) \quad \text{.....(2.70)}$$

The charge of the electron is (e), the group velocity is v_g. i.e. the velocity of electron, and $\partial n/\partial E$ is density of states per unit length in the lead in the energy window that can be determined by the chemical potentials from contacts:

$$\frac{\partial n}{\partial E} = \frac{\partial n}{\partial k} \frac{\partial k}{\partial E} = \frac{\partial n}{\partial k} \frac{1}{v_g \hbar} \quad \text{.....(2.71)}$$

As in one-dimension, after including a factor of 2 of the rotation dependency $\frac{\partial n}{\partial k} = \frac{1}{\pi}$. When we substitute into equation (2.71), we will find that $\frac{\partial n}{\partial E} = \frac{1}{\pi}\frac{1}{v_g \hbar}$, which simplifies the equation (2.70) to:

$$\delta I = \frac{2e}{h}(\mu_L - \mu_R) = \frac{2e^2}{h}\delta V \qquad \text{.....(2.72)}$$

Where δV is the voltage generated by the chemical potential mismatch. From Eq.(2.72) it is clear that in the absence of a scattering region, the conductance of a quantum wire with one open channel is $\frac{2e^2}{h}$. If now we consider a scattering region, the current collected in the right contacts will be:

$$\delta I = \frac{2e^2}{h} T(\mu)\delta V \implies \frac{\delta I}{\delta V} = G = \frac{2e^2}{h} T(\mu) \qquad \text{.....(2.73)}$$

This equation is the Landauer formula, which relates the conductivity G of a mesoscopic scatterer to the transmission probability T of the electrons passing through it. Where $T(\mu)$ is the transmission coefficient as a function of the chemical potential μ and the quantum conductance G_0 represented by $2e^2/h$. The quantity G_0 includes the factor of 2 in the formula to include spin degeneracy [114,140].

Landauer's formula has been generalized in more than one open case Buttiker channel [141]. In this case, the transmission coefficient is replaced by the sum of all the transmission amplitudes describing electrons coming from the left-hand contact and arriving to the right contact. Landauer's formula (Eq. 2.73) for many open channels and then it becomes:

$$\frac{\delta I}{\delta V} = G = \frac{2e^2}{h}\sum_{i,j}\left|t_{i,j}\right|^2 = \frac{2e^2}{h} Tr(tt^{\dagger}) \qquad \text{.....(2.74)}$$

Here, $t_{i,j}$ represents the transmission amplitude that describes the scattering from j[th] channel from the left leads to i[th] channel is for the right lead and G is the electric conductance. According to the definition of transmission amplitude, reflection amplitudes $r_{i,j}$ can be entered to describe the scattering processes where the particle is scattered to the same lead from which it came, here $r_{i,j}$ distinguish probability a particle arriving at channel j is reflected back on channel i of the same lead. By combining the transmission and reflection amplitudes, we can produce the scattering matrix we call the S matrix, which connects the states coming from the left lead to the right and vice versa as follows:

$$S = \begin{pmatrix} r & t' \\ t & r' \end{pmatrix} \qquad \text{.....(2.75)}$$

In this equation, r and t denote left-handed electrons, while r' and t' denote right-handed electrons. When we return to (Eq 2.74), we see that r, t, r', and t' are matrices of multiple open channels that can be complicated in the presence of a magnetic field. The following section calculates S for the system's retarded Green function G(E). G(E) is derived by coupling the Green function of the leads to the Green function of the scattering region using Dyson's equation. The S matrix is an important component of scattering theory. In other words, it is useful not only in describing linearity transport, but also in other problems such as adiabatic pumping [139,140].

3-1 Introduction

In molecular electronics, the aim is to understand electrical properties of molecular junctions; where a molecule (or sufficiently small structure) is bound to bulk electrodes so that ballistic transport can occur through its energy levels. The coupling strength between the leads and the molecule is usually small compared to the intra-electrode or intra-molecule bond strengths, which introduces a scattering process from the electrode to the molecule and from the molecule to the electrode. Since this system is not periodic, the electronic properties are no longer well described by the band structure, as calculated by the DFT method in Chapter 2. For this reason, a general approach is needed to understand the scattering process in the electrode junction and the molecular bridge. This can be achieved through the Green's function formalism.

3-2 Theoretical Building and Configuration:(Avogadro program)

To obtain the structure of all the systems in the thesis, the Avogadro program is used. Avogadro is an advanced molecular editor and visualizer designed for cross-platform use in computational chemistry, molecular modeling, bioinformatics, materials science and related fields (Figure 3-1).

It provides high-quality flexible rendering and a robust additional structure [141]. Avogadro offers a semantic chemical generator and platform for visualization and analysis. For users, it offers an easy-to-use generator, integrated support for downloading from popular databases such as Pub-Chemistry and Protein Data Bank, extraction of chemical data from a variety of formats, including computational chemistry output, and native semantic

support for the CML file format. For more theoretical details about Avogadro and what it offers, see [142].

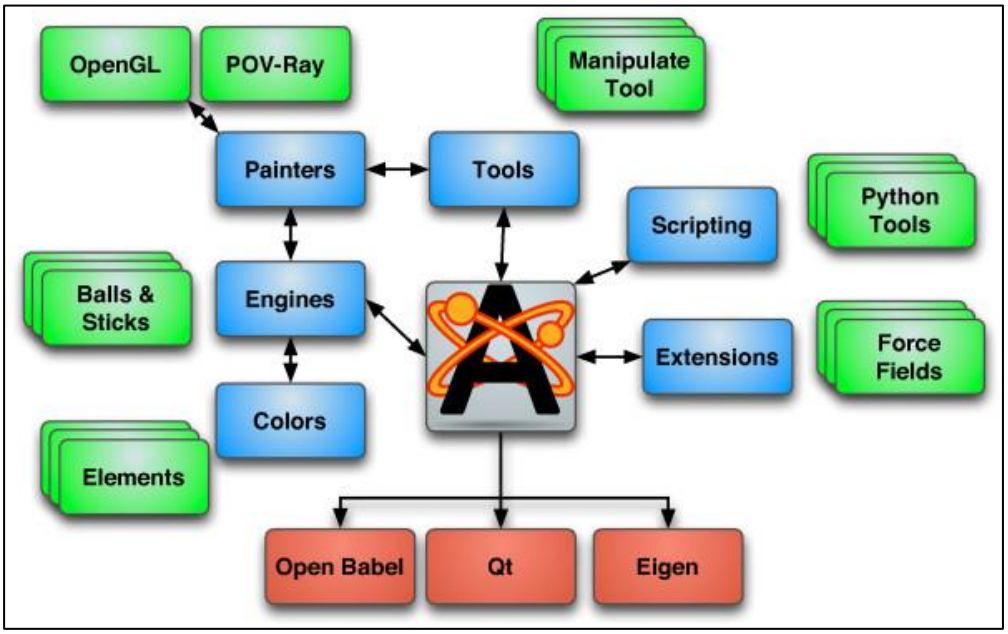

Figure(3-1) : Atomic building capabilities and tools using Avogadro[142].

3-3 Calculations of electrical and thermoelectric properties

To determine the electrical conductivity of the molecular, it is placed between two pyramidal gold electrodes and then allowed to relax to form the necessary shapes.

The transmission coefficient of a structure can be defined as the amplitude and intensity of the transmitted wave in comparison to the incident wave when waves propagate in a non-contact medium [99]. In non-relativistic quantum mechanics, the transmission coefficient and its corresponding reflection coefficient are used to describe the behaviour of a wave incident on a barrier. The transfer coefficient quantifies the likelihood of a particle tunnelling through a barrier. The transmission coefficient expresses the

probability flow of the transmitted wave in comparison to the incident wave's flow [143,144].

The structure's transmission coefficient is positioned between two electrodes. T(E) is a transmission coefficient that quantifies the transfer of energy from E electrons to another electrode. The Hamiltonian H and the interference matrices S [144] were used to determine T(E).

T(E), which characterizes the spread of energy electrons from left to right electrode, was determined by first collecting their Hamiltonian and related nested matrices using SIESTA and then using and Gollum's code [145,146] to calculate T(E) using the relationship:

$$T = Trace\{\Gamma_R(E)G^R(E)\Gamma_L(E)G^{R\dagger}(E)\} \quad \text{..... (3.1)}$$

In this expression,

$$\Gamma_{L,R}(E) = i\left(\sum_{L,R}(E) - \sum_{L,R}{}^{\dagger}(E)\right) \quad \text{..... (3.2)}$$

Equation (3.2) describes the level broadening due to the coupling between left (L) and right (R) electrodes and the central scattering region, $\sum_{L,R}(E)$ are the retarded self-energies associated with this coupling and:

$$G^R = (ES - H - \sum_L - \sum_R)^{-1} \text{..... (3.3)}$$

G^R is the retarded Green's function, where *H* is the Hamiltonian and *S* is the overlap matrix (both obtained from SIESTA). Electrical conductivity means flow of electric current through a material. When a current of one Ampere passes through a component across which a voltage of one Volt

exists, then the electrical conductance ($G = I/E$) of the component is one Siemens (S) [140, 147].

The electrical conductance *G(T)* and the thermopower as a function of the temperature T was computed from the formula:

$$L_n^{\sigma}(T) = \int_{-\infty}^{\infty}(E - E_F)^n \, T^{\sigma}(E) \left(-\frac{df(E)}{dE}\right) dE \qquad \ldots\ldots\ldots\ldots (3.4)$$

Where

$$f(\mathrm{E}) = [e^{\beta(E-E_F)} + 1]^{-1}. \qquad \ldots\ldots\ldots\ldots (3.5)$$

where $T^{\sigma}(E)$ is the transmission coefficient, and σ represents spin [↑, ↓] of transport of electrons passing through the single-molecule from one electrode to another [148], *F (E)* is the Fermi distribution function, $\beta = 1/k_B T$, E_F is the Fermi energy, k_B is Boltzmann constant, *T* is the temperature. The electrical conductance *G(T)* has been calculated by using Landauer formula:

$$G = G_o \int_{-\infty}^{\infty} dE \; T(E)[-df(E)/dE] \qquad \ldots\ldots\ldots\ldots (3.6)$$

Substitute an equation (3.4) into an equation (3.6) we get:

$$G(T) = G_{\circ} L_{\circ}(T) \qquad \ldots\ldots\ldots\ldots (3.7)$$

where

$$G_0 = \left(\frac{2e^2}{h}\right) \qquad \ldots\ldots\ldots\ldots (3.8)$$

Is the quantum of conductance, h is the Planck's constant, e is the electron charge. Since the quantity (*-df(E)/dE)* is the a probability distribution peaked at

$E = E_F$ with a width on the order K_BT, the previous expression shows that G/G_o is obtained by averaging T(E) over an energy range on the order K_BT in the vicinity of $E = E_F$[148,149]. It is well known that the Fermi energy predicted by DFT is not reliable, and therefore, the plots G/G_o have been shown later as a function of $E_F - E_F^{DFT}$. Then, the thermopower *S*(T) is given by[150,151]:

$$S(T) = -\frac{L_1}{eTL_\circ} \qquad \text{.....(3.9)}$$

3-3-1 Thermoelectric coefficients

When a system is subjected to a temperature difference ΔT and a voltage difference ΔV, the thermoelectric effect occurs. This results in the passage of an electric current I and a heat current $\dot{Q}$ through a device. According to Buttiker, Imry, Landauer, et al. [149-152], the electric current I and heat current $\dot{Q}$ passing through a device are proportional to the voltage difference ΔV and temperature differential ΔT. Thus, the thermoelectric coefficients G, L, M, and K are used to connect both currents to temperature and potential differences [150]:

$$\begin{pmatrix} I \\ \dot{Q} \end{pmatrix} = \begin{pmatrix} G & L \\ M & K \end{pmatrix} \begin{pmatrix} \Delta V \\ \Delta T \end{pmatrix} \qquad \text{.....(3.10)}$$

We can write the equation in another form:

$$\begin{pmatrix} I \\ \dot{Q} \end{pmatrix} = \frac{1}{h} \begin{pmatrix} e^2 L_o & \frac{e}{T} L_1 \\ eL_1 & \frac{1}{T} L_2 \end{pmatrix} \begin{pmatrix} \Delta V \\ \Delta T \end{pmatrix} \qquad \text{.....(3.11)}$$

Here, T represents the reference temperature, as well as the transport at room temperature through the single molecules are coherent in phase, with moments $L_n = L_n^{\uparrow} + L_n^{\downarrow}$. (n = 0,1,2), where L_n is written as (3.7).

We can rewrite equation (3.11) in the terms of the electrical conductance (G) (electrical resistance $R = 1/G$), thermopower ($S = -\Delta V/\Delta T$) , Peltier coefficient (Π), and the electronic contribution to the thermal conductance (k_e), as shown:

$$\begin{pmatrix} \Delta V \\ \dot{Q} \end{pmatrix} = \begin{pmatrix} \frac{1}{G} & -\frac{L}{G} \\ \frac{M}{G} & K - \frac{LM}{G} \end{pmatrix} \begin{pmatrix} I \\ \Delta T \end{pmatrix} = \begin{pmatrix} R & S \\ \Pi & k_e \end{pmatrix} \begin{pmatrix} I \\ \Delta T \end{pmatrix} \quad \text{.....(3.12)}$$

The electrical conductance, G is given by the Landauer formula: $G(T) = \left(\frac{2e^2}{h}\right) L_{\circ}(T)$,This parameter is described in an equation (3.10).

Thermal energy is given in this case: Seebeck's modulus is a measure of how much of the thermoelectric potential is induced in response to temperature difference across a substance. It can also be defined as the thermal energy and thermoelectric sensitivity of a material, and is measured in volts per kelvin (V/K) in SI units. The Seebeck modulus of a substance is calculated from equation (3.12) when a small temperature gradient is applied to a substance such as [153]:

$$S = -\frac{\Delta V}{\Delta T} = \frac{1}{eT} \frac{L_1}{L_o} \quad \text{.....(3.13)}$$

where ΔT is the small temperature difference between the two ends of a material and ΔV is the thermoelectric voltage visible at the ends.

Furthermore, the Peltier modulus is the inverse of the Seebeck modulus, as it is determined by flowing current through two junctions, resulting in a temperature difference. The Peltier effect was discovered in 1834 by physicist Peltier. This is not the same as Joule heating, despite appearances. In joule heating, the current simply raises the temperature of the material through which it passes, whereas in Peltier effect devices, a temperature differential is generated, with one junction being colder and the other becoming hotter. Peltier coolers, while not as efficient as some other types of coolers, are precise and simple to control and adjust. Peltier effect devices are used in a variety of microelectronic devices, including microcontrollers and central processing units in computers (CPUs). The Peltier effect occurs when an electric charge flows through a junction between two different conductors and generates or absorbs heat [18]. It is mostly used by computer enthusiasts to bypass microprocessors in order to increase performance without triggering CPU overheating or process failures. The Peltier coefficient is defined as the amount of heat that is transported solely as a result of the charge current in the absence of a temperature difference:

$$\Pi = \left(\frac{\dot{Q}}{I}\right)_{\Delta T=0} = \frac{1}{e}\frac{L_1}{L_o} = -ST \qquad \text{.....(3.14)}$$

And the electronic contribution to the thermal conductance (k_e) (and the thermal conductance k_e is defined as the heat current due to the temperature drop in the absence of an electric current) is given:

$$k_e = -\left(\frac{\dot{Q}}{\Delta T}\right)_{I=0} = \frac{1}{hT}\left(L_2 - \frac{L_1^2}{L_o}\right) = -K\left(1 + \frac{S^2\,GT}{K}\right) \qquad \text{.....(3.15)}$$

Therefore the evaluation of *S* or Π gives an idea of how well the device will act as a heat driven current generator or a current driven cooling device. An additional quantity, the thermoelectric figure of merit, *ZT* [151] can also be defined in terms of these measurable thermoelectric coefficients, from the above equations, the figure of merit $ZT = \frac{S^2\, GT}{K}$ can be written as:

$$ZT_e = \frac{1}{\frac{L_O L_2}{L_1^2} - 1} \qquad \text{……..(3.16)}$$

From classical electronics, *ZT* is derived by finding the maximum induced temperature difference produced by an applied electrical current in the presence of Joule heating. Let us consider a current carrying conductor placed between two heat paths with temperatures T_L and T_R, and electrical potentials V_L and V_R respectively. The thermoelectric figure of merit can be determined by finding the maximum induced temperature difference of the conductor due to an electrical current. Define $\dot{Q}$ as the heat gain from the path *L* to *R*, and then from Eq. (3.12) i.e.:

$$\dot{Q} = \Pi\, I - K\, \Delta T \qquad \text{…….(3.17)}$$

$\dot{Q}$ This heat transfer will cause the left path to be cold and the right path to be hot heat, with a result that ΔT increases. The amount of Joule heating can be expressed as $\dot{Q_J} = R\, I^2$, which is proportional to the electrical resistance and the square of the current. This Joule heating will also affect the temperature difference induced by the heat transfer, and therefore in the steady state case[152]

$$\Pi\, I - K\, \Delta T = \frac{R\, I^2}{2} \qquad \text{……(3.18)}$$

where, $R/2$ is the sum of two parallel resistances (internal and external resistances). After rearranging this, the temperature difference is:

$$\Delta T = \frac{1}{K}\left(\Pi I - \frac{R I^2}{2}\right) \quad \text{.....(3.19)}$$

This expression shows how the temperature difference depends on the current. To find the maximum temperature difference a differentiation Eq. (3.19) with respect to the electric current is made:

$$\frac{\partial \Delta T}{\partial I} = \frac{\Pi - IR}{k} = 0 \quad \text{.....(3.20)}$$

Finally by writing back $I = \Pi/R$ and substituting Eq. (3.14) into Eq. (3.19), for the maximum of the temperature different we get[154,156]:

$$(\Delta T)_{max} = \frac{\Pi^2}{2kR} = \frac{S^2 T^2 G}{2k} \quad \text{.....(3.21)}$$

$$\frac{(\Delta T)_{max}}{T} = \frac{S^2 T^2 G}{2k} = \frac{1}{2} ZT \quad \text{.....(3.22)}$$

$$\therefore ZT = \frac{2 S^2 T^2 G}{2K} \quad \text{.....(3.23)}$$

Yielding a dimensionless number that can be used to characterize the efficiency of a molecular device.

3-4 Electronic, Optical and Spectral Calculations

3-4-1 HOMO, LUMO and H-L Gap

The most significant molecular orbitals are HOMO and LUMO, where HOMO denotes the highest occupied molecular orbital and LUMO denotes the lowest unoccupied molecule orbital. The most significant molecular MOs orbitals are referred to as frontier orbitals since they are found at the molecules' electrons' extremes. HOMO, the highest energy orbital containing electrons, is the electron donor orbital. LUMO, on the other hand, is the lowest energy orbital with space for electrons. The energy (H-Lgap) is defined as [104,155]: the difference in energies between the HOMO and LUMO levels.

$$(H-L)_{E\ gap} = E_{HOMO} - E_{LUMO} \quad \text{..... (3.24)}$$

Not only do HOMO and LUMO and their associated energy gap determine the method by which molecules interact with other species, but the energy gap also helps characterize the chemical reaction and kinetic stability of the molecule. A molecule with a small frontier orbital gap is highly polarizable and is often associated with strong chemical reactivity and low kinetic stability; this type of molecule is sometimes referred to as a soft molecule [155,156]. When an electron is transported to a higher energy state, there by filling the empty molecular orbitals, the ensuing state is referred to as the excited state (Figure 3-2). The energy difference between the HOMO and LUMO states is referred to as the HOMO - LUMO gap [155].

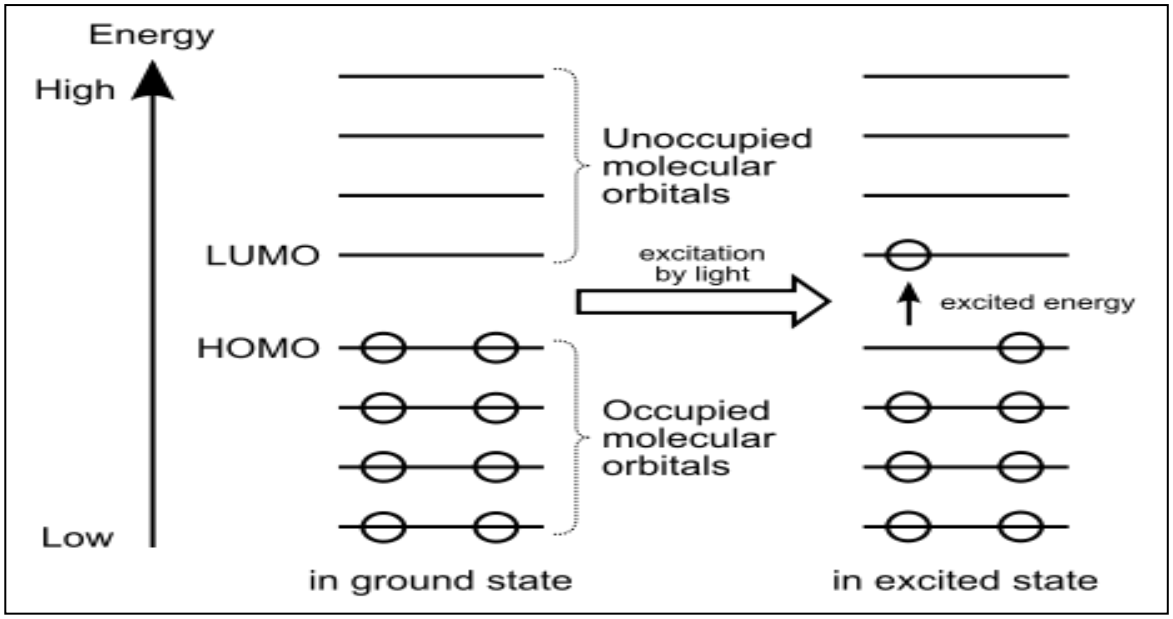

Figure (3-2): HOMO and LUMO levels of a single molecule[155].

The circle represents an electron in an orbital when light of a high enough frequency is absorbed by an electron in the HOMO, it is excited to the LUMO.

3.4.2 Fermi energy and Fermi level

The Fermi energy is a quantum mechanical notion that often refers to the energy difference between the highest and lowest occupied single-particle states in a quantum system of non-interacting fermions at absolute zero temperature. The lowest occupied state in a Fermi gas is assumed to have zero kinetic energy, but the lowest occupied state in a metal is commonly regarded to be the bottom of the conduction band [103]. Intriguingly, the word "Fermi energy" is frequently used interchangeably with another but closely related notion, the Fermi level (also called electrochemical potential), there are some critical distinctions between the Fermi level and Fermi energy, at least in the context of this article. While the Fermi energy is specified exclusively at

absolute zero, the Fermi level is defined at any temperature. The Fermi energy is a difference in energy levels (often equal to kinetic energy), whereas the Fermi level is a total energy level that includes both kinetic and potential energy. The Fermi energy can be defined only for non-interacting fermions (for which the potential energy or band edge is a static, well-defined quantity), whereas the Fermi level (for which the electrochemical potential of an electron remains well defined even in complex interacting systems at thermodynamic equilibrium) cannot be defined equilibrium.

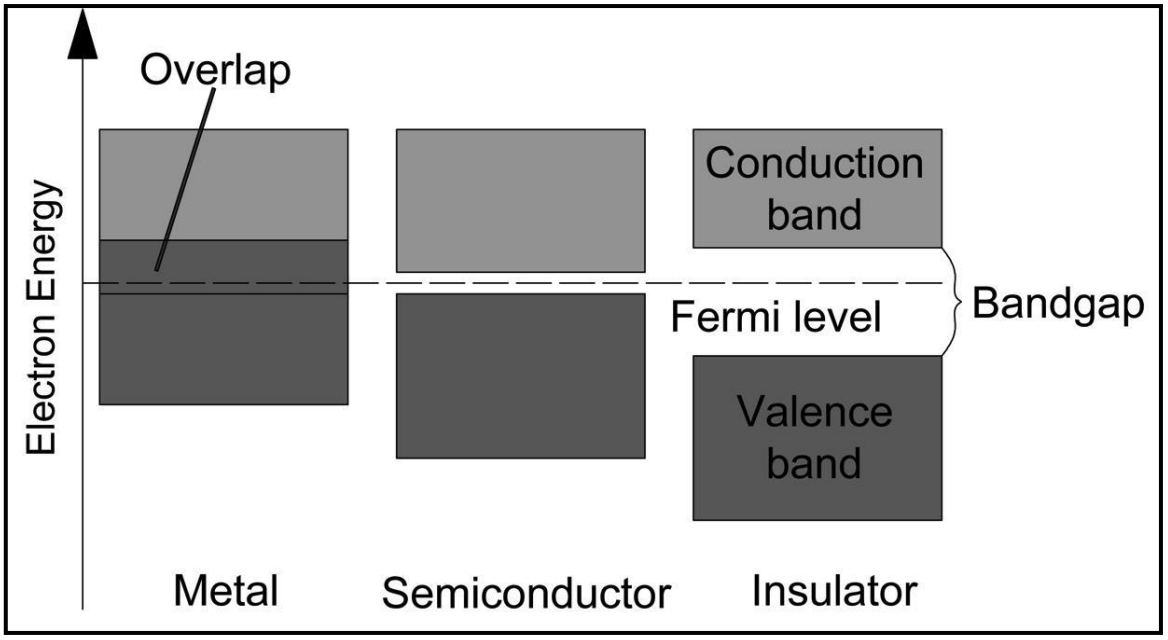

Figure (3-3): Fermi energy level of the metal, semiconductor and insulator[103].

Given that the energy of the highest occupied single particle state in a metal at absolute zero is the Fermi level, the Fermi energy in a metal is the energy difference between the Fermi level and the lowest inhabited single particle state at zero temperature, as seen in figure (3-3). Fermi energy level at temperature is given by: $F(\mathrm{E}) = [e^{\beta(E-E_F)} + 1]^{-1}$ Where f (E) is the Fermi

function, $\beta = 1/k_B T$, E_F is the Fermi energy, k_B is Boltzmann constant, T is the temperature.

The Fermi energy, which is the fundamental anisotropy principle in DFT, is utilized to determine the direction of an electron cloud's departure. It is constant over all dimensions and may be calculated using the following equation [157]:

$$E_F = \left[\frac{\partial E}{\partial N}\right] v_{(\vec{r})} \quad \text{.....(3.25)}$$

Where E is the energy and N is the number of electrons. Theoretically, Fermi energy is relating as in the following equation [160]:

$$E_F \approx \frac{1}{2} (E_{HOMO} + E_{LUMO}) \quad \text{.....(3.26)}$$

Band theory can be used to explain the electrical conductivity of materials. In band theory, each electron's energy level is represented by a horizontal line. Due to the fact that any solid substance has a significant number of electrons with varying energy levels, the combinations of these energy levels form two continuous energy bands referred to as the valence band and the conduction band. The energy difference between the two bands denotes the electron-restricted zone. In band theory, the electrons bound to particular atoms or interatomic bonds are considered to be in the valence band. When an electric field is applied, electrons that may freely flow within the core are said to be in the conduction band. The pattern of bands in a solid in Figure (3.3) identifies three distinct types of materials: insulators, semiconductors, and metals.

3-4-3 Electronic Transitions

UV or visible ray absorption results in the stimulation of external electrons. There are three types of electronic transitions: those involving p, s, and n electrons, those involving charge transfer electrons, and those involving d and f electrons. When an atom or molecule absorbs energy, the electrons in its ground state are promoted to the excited state. Atoms in a molecule can rotate and vibrate in relation to one another. Additionally, these vibrations and rotations have distinct energy levels, which might be thought of as a dense existence atop each electrical level. UV and visible rays are absorbed by some functional groups in organic compounds that contain valence electrons with a low excitation energy. The spectrum of the chromosphere-containing molecule is complicated [158,159]. The electronic transitions between p, s, and n electrons are depicted in (Fig. 3-4).

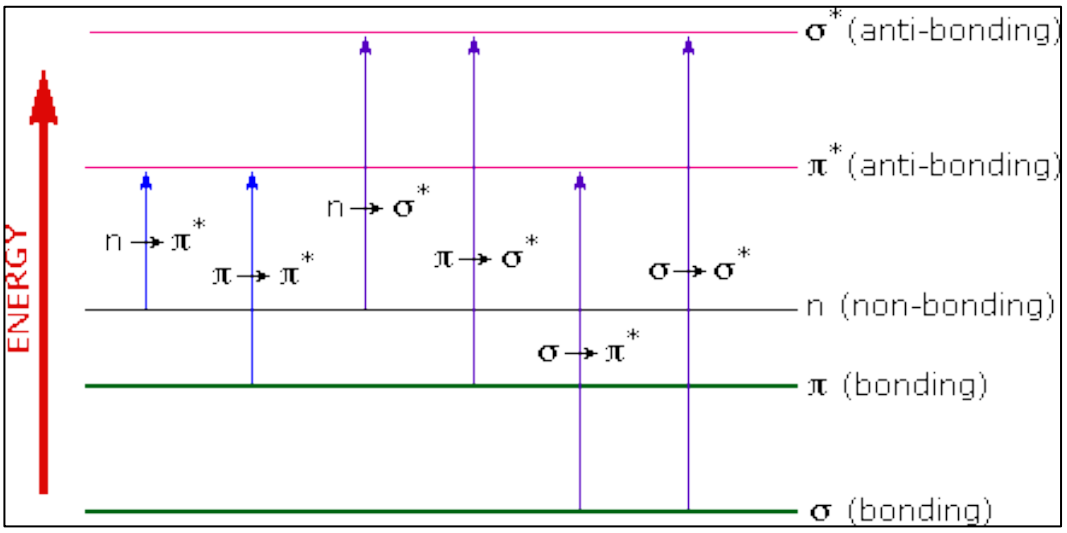

Figure (3-4): The electronic transitions of p, s, and n electrons [159].

3-5 Self-Consistency Process

After establishing the system's atomic configuration, we require the appropriate pseudo-potentials for each element, which can vary for each cross-correlation function. Additionally, a suitable base set selection must be made for each item in the account.

In the event of comprehensive optimization, the three alternatives can be combined to obtain the system's least energy and equilibrium network parameters. The process for relaxing the atomic locations allows the atoms to migrate until the remaining force between all the atoms is less than the needed affinity tolerance in eV/, as seen in (Figure 3-5). Force is the essential quantity in structural optimization, and it may be numerically determined by taking the approximate numerical derivatives of the total power with respect to positions. SIESTA implements this strategy using the Hellmann-Feynman theorem [141,142]. We can enhance the computational accuracy and cost by doing two test calculations. Other input parameters affect the calculation's accuracy, such as the precision and density of the k-grid points used to evaluate the integration. Then, assuming that there is no interaction between the atoms, we generate the initial charge density.

Due to the fact that the pseudopotentials are known, this step is straightforward, and the total charge density is equal to the sum of the atomic densities. The self-consistent computation (Figure 3-5) begins with the Hartree-potential and exchange correlation potentials being calculated. Due to the fact that the density is represented in real space, the Hartree-potential is determined by solving the Poisson equation using either the multiple mesh approach [148] or the rapid Fourier transform method [102]. We begin the

next iteration after solving the Kohn-Sham equations and obtaining a new density (r). Iteration is complete when the required convergence requirements are met. SIESTA offers extra density matrix mixing choices per cycle. I employ the Pulay [141] mixing approach in particular, in which the new density is mixed not just with the old, but also with a linear mixture of the preceding n densities. As a result, we obtain the ground state Kohn-Sham orbitals and energy of a certain atomic arrangement. The operation described above is repeated in another loop, which is controlled by the conjugate gradient method [141,142], which is used to determine the minimal ground state energy and related atomic configuration. After achieving self-consistency, an additional subroutine is called to extract the Hamiltonian and nested matrices from the LCAO basis for use in scattering calculations.

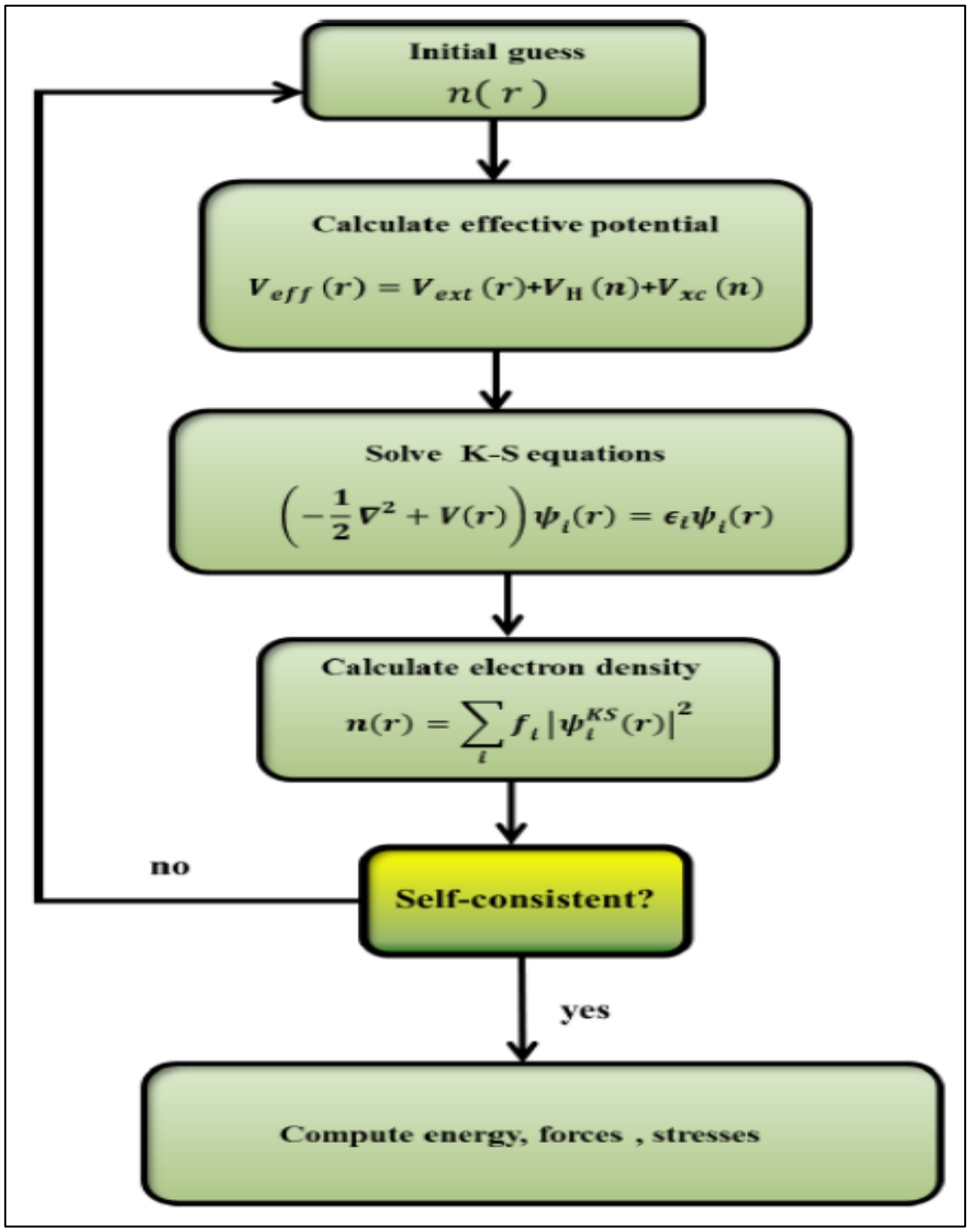

Figure (3-5): Schematic of the self-consistency process within SIESTA[142].

3-6 The Programs

The method presented so far in this chapter is quite powerful, and has been used in many areas of mesoscopic transport in the last decade. It has been successfully applied to molecular electronics [160,161,162], spintronics [163,164] and mesoscopic superconductivity [165-166]. The method has also been extended for finite bias employing the non-equilibrium Green's function technique [167]. A Hamiltonian, which describes our system, can be created manually or can be an output of a numerical calculation, such as HF, DFT code or density functional tight-binding method. In this section, a theoretical background of the steps, procedures and computational programs that used to calculate the electronic, thermoelectric, optical, spectral and structural properties of all systems under investigation in this thesis.

3-6-1 SIESTA

All calculations were carried out by the implementation of DFT in the SIESTA code. It is used to obtain the relaxed geometry of the discussed structures and also to carry out the calculations to investigate their electronic properties. SIESTA is an acronym derived from the Spanish Initiative for Electronic Simulations with Thousands of Atoms. It is a self-consistent density functional theory technique which uses norm-conserving pseudo-potentials and a Linear Combination of Atomic Orbital Basis set (LCAOB) to perform efficient calculations [168]. The SIESTA code is used to obtain the ground state energy of different atomic configurations, and then obtain the relaxed structure of the systems. This means that SIESTA can provide us the energy as a function of the atomic coordinates (position of atoms) [169]. The structure optimization (also known as geometry optimization) contains three

options; relaxing atomic coordinates, allowing periodic cell shapes and volumes to change. In case of full optimization, the three options can be employed together, which leads to the minimum energy of the atoms in the system and the equilibrium lattice parameters of the systems. Performing the relaxation of the atomic positions allows atoms to move until the residual force between all atoms is smaller than the required convergence tolerance in eV/Å, as shown in Figure 3.5. In structural optimization the force is the key quantity and this force could be calculated numerically by taking the approximate numerical derivatives of the total energy with respect to the positions. This method is applied in SIESTA using the Hellmann-Feynman theorem [170]. There are two different modes to perform DFT simulations using SIESTA one a conventional self-consistent field diagonalisation method to solve the Kohn-Sham equations and two by direct minimization of a modified energy functional.

3-6-2 GOLLUM Code

GOLLUM is a program written by Fortran that computes the electrical and thermal transport properties of multi-terminal nano-scale systems. The program can compute transport properties of either user-defined systems described by a tight-binding (or Huckel) Hamiltonian. The program has been created to interface easily with any DFT code and uses a localized basis [150]. It currently reads information from SIESTA [147]. Plans to produce interfaces to other codes like FIREBALL are underway. GOLLUM is based on equilibrium transport theory, meaning that it consumes much less memory than NEGF (non-equilibrium Greens function) codes. The program has been designed for user-friendliness and takes a considerable leap towards the

realization of ab initio multi-scale simulations of conventional and more sophisticated transport functionalities. GOLLUM delivers functionalities, reads either Tight-Binding or DFT Hamiltonians, simulates multi-terminal devices, computes the full scattering matrix and charge transport, number of open scattering channels, transmission and reflection coefficients, shot-noise, computes heat transport, thermal conductance and thermo power (Seebeck coefficient), peltier coefficient, computes spin transport, computes zero-voltage as well as I-V curves, computes band-structure of the leads and DOS in the scattering region [146,153,171].

3-6-3 Gaussian Code

Gaussian Code is a very high-end quantum chemical software package, available commercially through Gaussian, Inc. The Software runs on virtually all computer platforms, including Microsoft Windows. In addition, it can be accessed through Web based, interface tools such as Web MO. Gaussian is the most powerful software available to, educators and student researchers through the North Carolina School Computational, Chemistry server. Currently, Gaussian09 (G09) is available. The "09" refers to the year 2009 in which the software was published. G09 is not the most recent version [172].

References

[1] M. Di Ventra, S. Evoy and J. R. Heflin, “Introduction to Nanoscale Science and Technology”, Series: Nanostructure Science and Technology, Springer, p. 611, (2004).

[2] U. M. Ravaioli, “Computational Nanotechnology: Simulation of Nanoscale Electronic Systems”, Department of Electrical and Computer Engineering University of Illinois at Urbana-Champaign Urbana, IL 61801 USA (2007).

[3] A. Nitzan, “Electron transmission through molecules and molecular interfaces”, Annual Review Physical Chemistry, Vol. 52, pp. 681–750, (2001).

[4] K. Manabu, ed. Single-Molecule Electronics: An Introduction to Synthesis, Measurement and Theory. Springer, (2016).

[5] R. Martel, T Schmidt, HR Shea, T Hertel., "Single- and multi-wall carbon nanotube field-effect transistors". Applied Physics Letters, 73(17): p. 2447-2449,(1988).

[6] A. DeHon, Array-based architecture for FET-based, nanoscale electronics. IEEE Transactions on Nanotechnology, 2(1):p. 23-32,(2003).

[7] Z. Donhauser, J., A. Mantoothk, F. Kellyl,A. Bummj,D. Monnellj, J. Stapeltond, W. Price, JR.A. M. Rawlettd, L. Allaraj, M. Tour and ,P. S. Weiss, "Conductance Switching in Single Molecules Through Conformational Changes". Science, 292(5525): p. 2303,2001.

[8] C. Wang, , Yongjie Hu, Charles M. Lieber, and Shouheng Sun., "Ultrathin Au nanowires and their transport properties. J Am Chem Soc", 130(28): p. 8902-3,(2008).

[9] M. Tsutsui, and M. Taniguchi, Single Molecule Electronics and Devices. Sensors (Basel, Switzerland), 12(6): p. 7259-7298,(2012).

[10] R. Waser, and M. Aono, Nanoionics-based resistive switching memories. Nature Materials, 6: p. 833,(2007).

[11] D. Paul Franzon ,David P. ,Nackashi Christian J. Amsinck Sachin Sonkusale., "Molecular Electronics – Devices and Circuits Technology, in Vlsi-Soc: From Systems To Silicon: Proceedings of IFIP TC 10, WG 10.5", Thirteenth International Conference on Very Large Scale Integration of System on Chip (VLSI-SoC 2005), October 17-19, 2005, Perth, Australia, R. Reis, A. Osseiran, and H.-J. Pfleiderer, Editors. Springer US: Boston, MA. p. 1-10. 26.2007.

[12] M. NCPetty, Molecular Electronics, in Springer Handbook of Electronic and Photonic Materials, S. Kasap and P. Capper, Editors. Springer International Publishing: Cham. p. 1-1,2017.

[13] M. Ratner, “A brief history of molecular electronics,” Nat. Nanotechnol., vol. 8, no. 6, pp. 378–381, 2013.

[14] R. A. Marcus, “Electron transfer reactions in chemistry. Theory and experiment,” Rev. Mod. Phys., vol. 65, no. 3, p. 599, 1993.

[15] R. Chau, B. Doyle, S. Datta, J. Kavalieros, and K. Zhang, “Integrated nanoelectronics for the future,” Nat. Mater., vol. 6, no. 11, pp. 810–812, 2007.

[16] J. R. Heath and M. A. Ratner, “Molecular electronics,” 2003.

[17] D. Q. Andrews, G. C. Solomon, R. P. Van Duyne and M. A. Ratner, “Single Molecule Electronics: Increasing Dynamic Range and

Switching Speed Using Cross-Conjugated Species", Journal American Chemical Society, Vol. 130(51), pp. 17309-17319, (2008).

[18] M. Famili, I. M. Grace, Q. Al-Galiby, H. Sadeghi and C. J. Lambert, "Toward High Thermoelectric Performance of Thiophene and Ethylenedioxythiophene (EDOT) Molecular Wires", Advanced Functional Material, Vol. 28(15), (2018).

[19] V.M. Garcia-Suarez, C.J. Lambert, D.Z. Manrique, and T. Wandlowski, "Redox control of thermopower and figure of merit in phase-coherent molecular wires", IOP Science, Nanotechnology, Vol. 25(20), (2014).

[20] I. Díez-Pérez, J. Hihath, Y. Lee, L. Yu, L. Adamska, M. A. Kozhushner, I. I. Oleynik and N. Tao, "Rectification and stability of a single molecular diode with controlled orientation", Journal Nature Chemistry, Vol. 1, pp. 635-641, (2009).

[21] S. Richter, E. Mentovich and R. Elnathan, "Realization of Molecular-Based Transistors", Article Advanced Materials, Literature Review, Vol. 30(41), (2018).

[22] A. Batra, P. Darancet, Q. Chen, J. S. Meisner, J. R. Widawsky, J. B. Neaton, C. Nuckolls and L. Venkataraman, "Tuning rectification in single-molecular diodes", Journal American Chemical Society, Nano Lett. Vol. 13(12), pp. 6233-6237, (2013).

[23] A. S. Blum, J. G. Kushmerick, D. P. Long, C. H. Patterson, J. C. Yang, J. C. Henderson, Y. Yao, J. M. Tour, R. Shashidhar and B. R. Ratna, "Molecularly inherent voltage-controlled conductance switching", Journal Nature Materials, Vol. 4, pp. 167-172, (2005).

[24] S. J. van der Molen, J. Liao, T. Kudernac, J. S. Agustsson, L. Bernard, M. Calame, B. J. Van Wees, B. L. Feringa and C. S. Schönenberger, "Light-controlled conductance switching of ordered metal-molecule-metal devices", Journal American Chemical Society, Nano Lett. Vol. 9(1), pp. 76-80, (2009).

[25] C. C. Jia, A. Migliore, N. Xin, S. Y. Huang, J. Y. Wang, Q. Yang, S. P. Wang, H. L. Chen, D. M. Wang, B. Y. Feng, Z. R. Liu, G. Y. Zhang, D. H. Qu, H. Tian, M. A. Ratner, H. Q. Xu, A. Nitzan and X. F. Guo, "Covalently bonded single-molecule junctions with stable and reversible photo-switched conductivity", Science, Vol. 352(6292), pp. 1443-1445, (2016).

[26] G. Yzambart, L. Rincón-Garcí, A. Alaa Al-Jobory, A. K. Ismael, G. Rubio-Bollinger, C. J. Lambert, N. Agraït and M. R. Bryce, "Thermoelectric Properties of 2,7-Dipyridylfluorene Derivatives in Single-Molecule Junctions", Journal American Chemical Society, Vol. 122(48), pp. 27198-27204, (2018).

[27] M.José Soler1, Emilio Artacho, Julian D Gale, Alberto García, Javier Junquera, Pablo Ordejón and Daniel Sánchez-Portal., "The SIESTA method for ab initio order-N materials simulation," J. Phys. Condens. Matter, vol. 14, no. 11, p. 2745, 2002.

[28] A. D. Becke, "Density-functional thermochemistry. I. The effect of the exchange-only gradient correction," J. Chem. Phys., vol. 96, no. 3, pp. 2155–2160, 1992.

[29] J.Ferrer, C. J Lambert, V. M García-Suárez, D. Zs Manrique, D. Visontai, L. Oroszlany, R. Rodríguez-Ferradás, I .Grace, S .W. D

Bailey,K. Gillemot, Hatef Sadeghi and L .A Algharagholy, "GOLLUM: a next-generation simulation tool for electron, thermal and spin transport," New J. Phys., vol. 16, no. 9, p. 93029, 2014.

[30] A. Geim, Novoselov, K. The rise of graphene. Nature Mater. 2007, 6(3), 183–191.

[31] D.R. Kauffman, D.C. Sorescu, D.P. Schofield, B.L. Allen, K.D. Jordan, A. Star Understanding the Sensor Response of Metal-Decorated Carbon Nanotubes ,Nano Lett. 2010, 10, 958.

[32] J.C. Ellenbogen, J.C. Love Architectures for molecular electronic computers. I. Logic structures and an adder designed from molecular electronic diodes,Proc. IEEE 2000, 88, 386.

[33] M. Baghernejad, Zhao, X.; Baruel Ornso, K.; Fueg, M.; Moreno-Garcia, P.; Rudnev, A. V.; Kaliginedi, V.; Vesztergom, S.; Huang, C.; Hong, W.; Broekmann, P.; Wandlowski, T.; Thygesen, K. S.; Bryce, M. R., Electrochemical Control of Single-Molecule Conductance by Fermi- Level Tuning and Conjugation Switching, J. Am. Chem. Soc. 136, 17922-17925,2015.

[34] Y. Geng, ,Sangtarash, S.; Huang, C.; Sadeghi, H.; Fu, Y.; Hong, W.; Wandlowski, T.; Decurtins, S.; Lambert, C. J.; Liu, S. X., Magic ratios for connectivity-driven electrical conductance of graphene-like molecules, J. Am. Chem. Soc. 137, 4469-4476.; Sangtarash, S.; Huang, C. Sadeghi, H.; Sorohhov, G.; Hauser, J.; Wandlowski, T.; Hong, W.; Decurtins, S.; Liu, S-X.; Lambert, C.J.; Searching the hearts of graphene- like molecules for simplicity, sensitivity, and logic, J. Am. Chem. Soc. 137 (35), 11425- 11431 (2015)

[35] G. Yang ; Wu, H.; Wei, J.; Zheng, J.; Chen, Z.; Liu, J.; Shi, J.; Yang, Y.; Hong, W., Quantum interference effect in the charge transport through single-molecule benzene dithiol junction at room temperature: An experimental investigation, Chin. Chem. Lett. 29, 147-150,2018

[36] X. Liu , Sangtarash, S.; Reber, D.; Zhang, D.; Sadeghi, H.; Shi, J.; Xiao, Z.-Y.; Hong, W.; Lambert, C. J.; Liu, S.-X., Gating of Quantum Interference in Molecular Junctions by Heteroatom Substitution, Angew. Chem. Int. Ed. 56, 173-176,2017.

[37] M. Kiguchi, Kaneko, S., Single molecule bridging between metal electrodes. Phys Chem Chem Phys **,** 15 (7), 2253-2267,2013.

[38] R.J. Nichols,; Higgins, S. J., Single-Molecule Electronics: Chemical and Analytical Perspectives. Annu Rev Anal Chem**,** 8, 389-417,2015.

[39] Y. Aeschi, Li, H.; Cao, Z.; Chen, S.; Amacher, A.; Bieri, N.; Oezen, B. Hauser, J.; Decurtins, S.; Tan, S.; Liu, S.-X., Directed metalation cascade to access highly functionalized thieno[2,3-f]benzofuran and exploration as building blocks for organic electronics, Org. Lett. 15, 5586-5589,2013.

[40] Yi, C. Y.; Blum, C.; Lehmann, M.; Keller, S.; Liu, S. X.; Frei, G.; Neels, A.; Hauser, J.; Schürch, S.; Decurtins, S., Versatile Strategy To Access Fully Functionalized Benzodifurans: Redox-Active Chromophores for the Construction of Extended π-Conjugated Materials, J. Org. Chem. 75, 3350-3357,2010.

[41] Y. Didane, Mehl, G. H.; Kumagai, A.; Yoshimoto, N.; Videlot-Ackermann, C.; Brisset, H., A “Kite” Shaped Styryl End-Capped

Benzo[2,1-b:3,4-b′]dithiophene with High Electrical Performances in Organic Thin Film Transistors, J. Am. Chem. Soc. **2008,** 130, 17681– 17683.

[42] H. Li, Tang, P.; Zhao, Y.; Liu, S.-X.; Aeschi, Y.; Deng, L.; Braun, J.; Zhao, B.; Liu, Y.; Tan, S.; Meier, W.; Decurtins, S., Benzodifuran-containing well-defined π-conjugated polymers for photovoltaic cells, J. Polym. Sci. Part A: Polym Chem, **2012**, 50, 2935-2943.

[43] Z.L.Cheng, Skouta, R.; Vazquez, H.; Widawsky, J. R.; Schneebeli, S.; Chen, W.; Hybertsen, M. S.; Breslow, R.; Venkataraman, L., In situ formation of highly conducting covalent Au-C contacts for single-molecule junctions, Nat. Nanotechnol. **2011,** 6, 353-357.

[44] W. Hong, Li, H.; Liu, S.-X.; Fu, Y.; Li, J.; Kaliginedi, V.; Decurtins, S.; Wandlowski, T., Trimethylsilyl-Terminated Oligo(phenylene ethynylene)s: An Approach to Single-Molecule Junctions with Covalent Au–C σ-Bonds, J. Am. Chem. Soc. **2012,** 134, 19425-19431.

[45] T. D. Lash, “Origin of aromatic character in porphyrinoid systems,” J. Porphyr. Phthalocyanines, vol. 15, no. 11n12, pp. 1093–1115, 2011.

[46] F. Chen, X. Li, J. Hihath, Z. Huang, and N. Tao, “Effect of anchoring groups on single-molecule conductance: comparative study of thiol-, amine-, and carboxylic-acid-terminated molecules,” J. Am. Chem. Soc., vol. 128, no. 49, pp. 15874–15881, 2006.

[47] K. M. Bichinho, G. P. Pires, J. H. Z. dos Santos, M. M. de Camargo Forte, and C. R. Wolf, “Determination of Mg, Ti and Cl in Ziegler-Natta catalysts by WDXRF,” Anal. Chim. Acta, vol. 512, no. 2, pp. 359–367, 2004.

[48] M. Pawlicki, H. A. Collins, R. G. Denning, and H. L. Anderson, "Two-photon absorption and the design of two-photon dyes," Angew. Chemie Int. Ed., vol. 48, no. 18, pp. 3244–3266, 2009.

[49] V. S. Lin, S. G. DiMagno, and M. J. Therien, "Highly conjugated, acetylenyl bridged porphyrins: new models for light-harvesting antenna systems," Science (80-.)., vol. 264, no. 5162, pp. 1105–1111, 1994.

[50] P. Taylor, R. Aplin, and H. Anderson, "Conjugated porphyrin oligomers from monomer to hexamer," Chem. Commun., no. 8, pp. 909–910, 1998.

[51] H. J. Hogben, J. K. Sprafke, M. Hoffmann, M. Pawlicki, and H. L. Anderson, "Stepwise effective molarities in porphyrin oligomer complexes: preorganization results in exceptionally strong chelate cooperativity," J. Am. Chem. Soc., vol. 133, no. 51, pp. 20962–20969, 2011.

[52] J. Song, N. Aratani, H. Shinokubo, and A. Osuka, "Pyrrole-Bridged Porphyrin Nanorings," Chem. Eur. J., vol. 16, no. 45, pp. 13320–13324, 2010.

[53] A. V Deshpande, A. Beidoun, A. Penzkofer, and G. Wagenblast, "Absorption and emission spectroscopic investigation of cyanovinyldiethylaniline dye vapors," Chem. Phys., vol. 142, no. 1, pp. 123–131, 1990.

[54] W. Huang,S. -Kyu Lee,Young Mo Sung,Fulei Peng,Dr. Bangshao Yin,Prof. Dr. Ming Ma,Prof. Dr. Bo Chen,Prof. Dr. Shubin Liu,Prof. Dr. Steven Robert Kirk,Prof. Dr. Dongho Kim,Prof. Dr. Jianxin Song., "Azobenzene-Bridged Porphyrin Nanorings: Syntheses,

Structures, and Photophysical Properties," Chem. Eur. J., vol. 21, no. 43, pp. 15328–15338, 2015.

[55] R. Davidson, A. Oday Al-Owaedi, David C. Milan, Qiang Zeng, Joanne Tory, František Hartl, Simon J. Higgins, Richard J. Nichols, Colin J. Lambert, and Paul J. Low, "Effects of electrode–molecule binding and junction geometry on the single-molecule conductance of bis-2, 2′: 6′, 2 ″-Terpyridine-based complexes," Inorg. Chem., vol. 55, no. 6, pp. 2691–2700, 2016.

[56] C. J. Lambert, "Basic concepts of quantum interference and electron transport in single-molecule electronics," Chem. Soc. Rev., vol. 44, no. 4, pp. 875–888, 2015.

[57] A. Oday Al-Owaedi, C. D. Milan, O. Marie-Christine, B. Sören, S. Y. Dmitry, A. K. Judith Howard, S. J. Higgins, R. J. Nichols, C. J. Lambert, M. R. Bryce and P. J. Low. "Experimental and Computational Studies of the Single-Molecule Conductance of Ru(II) and Pt(II) trans-Bis (acetylide) Complexes", Journal American Chemistry Society, Organometallics, Vol. 35(17), pp. 2944−2954, (2016).

[58] T. Markussen, Stadler, R.; Thygesen, K. S. The relation between structure and quantum interference in single molecule junctions. Nano Lett. 2010. 10(10): p. 4260–4265.

[59] A. Nataiya Zimbovskaya, R. pederson, Electron transport through molecular junctions, Physics Reports, 2011, 509, 1-87.

[60] P. Moreno-Garcia, M. Gulcur, D. Z. Manrique, T. Pope, W. Hong, / V. Kaliginedi, C. Huang, A. S. Batsanov, M. R. Bryce, C. Lambert and T. Wandlowski Single-molecule conductance of functionalized

oligoynes: length dependence and junction evolution , J. Am. Chem. Soc., 2013, 135, 12228-12240.

[61] H.-M. Wen ; Yang, Y.; Zhou, X.-S.; Liu, J.-Y.; Zhang, D.-B.; Chen, Z.-B. Wang, J.-Y.; Chen, Z.-N.; Tian, Z.-Q. Electrical conductance study on 1,3- butadiyne-linked dinuclear ruthenium(ii) complexes within single molecule break junctions. Chem. Sci. 2013. 4(6): p. 2471–2477.

[62] D. C. Milan, O. A. Al-Owaedi, M.-C. Oerthel, S. Marqués-González, R. J. Brooke, M. R. Bryce, P. Cea, J. Ferrer, S. J. Higgins, C. J. Lambert, P. J. Low, D. Z. Manrique, S. Martin, R. J. Nichols, W. Schwarzacher and V. M. García-Suárez, Solvent Dependence of the Single Molecule Conductance of Oligoyne-Based Molecular Wires J. Phys. Chem. C, 2015, DOI: 10.1021/acs.jpcc.5b08877.

[63] A. Oday Al-Owaedi, S. Bock, D. C. Milan, O. Marie-Christine, S. I. Michael, S. Y. Dmitry, N. S. Alexandre, J. L. Nicholas , T. Albrecht, J. H. Simon, R. B. Martin, J. N. Richard, C. J. Lambert and Paul J. Low. “Insulated molecular wires: inhibiting orthogonal contacts in metal complex based molecular junctions”, Journal Nanoscale, Vol. 9(28), pp. 9902–9912, (2017).

[64] P. Sam-ang and G. R. Matthew, “Characterizing destructive quantum interference in electron transport”, IOP Science, New Journal of Physics, Vol. 19, (2017).

[65] R. J. Davidson, D. C. Milan, O. A. Al-Owaedi, A. K. Ismael, R. J. Nichols, S. J. Higgins, C. J. Lambert, D. S. Yufita and Andrew

Beeby, “Conductance of ‘bare-bones’ tripodal molecular wires”, Journal RSC Advanced, Vol. 8(42), pp. 23585–23590, (2018).

[66] C. J. Judd “Molecular quantum rings formed from a π-conjugated macrocycle,” Phys. Rev. Lett., vol. 125, no. 20, p. 206803, 2020.

[67] A. A. Baraa Al-Mammory, A. Oday Al-Owaedi and M. Enas Al-Robayi, “Thermoelectric Properties of Oligoyne-Molecular Wires”, IOP Science, Journal of Physics: Conference Series, Vol. 1818(1), (2021).

[68] M. Rasool Al-Utayjawee and A. Oday Al-Owaedi, " Quantum Transport Properties of Single Organic Molecule as a Promising Candidate for Laser Active Medium" IOP Science Journal of Physics: Conference Series, Vol. 1818(1), (2021).

[69] I. O. Abbas and M. Enas Al-Robayi ,"Quantum Transport Properties of Organometallic Molecules Junction",Thesis, University of Babylon,(2022) .

[70] F. Schedin, A. K. Geim, S.V. Morozov, E. W. Hill, P. Blake, M. I.Katsnelson and K. S. Novoselov, “Detection of individual gas molecules adsorbed on grapheme”, Nature materials ,Vol. 6, pp. 652- 655, (2007).

[71] D. Young, “Computational Chemistry: A Practical Guide for Applying Techniques to Real World Problems”, Hand Book, 3rd Edition, Wiley & Sons, Inc., New York, p. 408, (2001).

[72] M. Mueller, “Fundamentals of Quantum Chemistry: Molecular Spectroscopy and Modern Electronic Structure Computations”,

Book, Springer, 1st Edition, Kluwer Academic/Plenum Publishers, New York, p. 278, (2001).

[73] C. J. Cramer, " Essentials of Computational Chemistry: Theories and Models", Book, 2nd Edition, John Wiley & Sons Ltd., The Atrium, Southern Gate, Chichester, England, p. 624, (2004). [42] N. Argaman and G. Makov, "Density functional theory: An introduction," Am. J. Phys., vol. 68, no. 1, pp. 69–79, 2000.

[74] C. L. Tang, "Fundamentals of Quantum Mechanics for Solid State Electronics and Optics", Book, 1st Edition, Cambridge University Press, NY publishes, Ithaca, p. 224, (2009).

[75] D.D. Fitts, "Principles of Quantum Mechanics: As Applied to Chemistry and Chemical Physics", Book, 1st Edition, Cambridge University Press, New York, p. 364, (1999).

[76] P. A. Cox, "introduction to Quantum Theory and Atomic Structure", Book, 1st Edition, Oxford University Press , New York, p. 96 (1996).

[77] D.W. Rogers, "Computational Chemistry Using the PC", Book, 3rd Edition., John Wiley & Sins, Inc., Hoboken, New Jersey, p.349 (2003).

[78] N. Argaman and G. Makov, "Density functional theory: An introduction," Am. J. Phys., vol. 68, no. 1, pp. 69–79, 2000.

[79] R. Dronskowski, "Computational Chemistry of Solid State Materials," Mater. Today, vol. 9, 2006.

[80] H. Eschrig, The fundamentals of density functional theory, vol. 32. Springer, 1996.

[81] R. G. Parr and W. Yang, “Density-functional theory of atoms and molecules. International Series of Monographs on Chemistry,” Oxford Univ. Press. New York, vol. 3, pp. 14312–14321, 1994.

[82] A. Kumar, “A Brief Introduction to Thomas-Fermi Model in Partial Differential Equations,” 2012.

[83] E. H. Lieb, “Erratum: Thomas-Fermi and related theories of atoms and molecules,” Rev. Mod. Phys., vol. 54, no. 1, p. 311, 1982.

[84] W. Kohn and L. J. Sham, “Self-consistent equations including exchange and correlation effects,” Phys. Rev., vol. 140, no. 4A, p. A1133, 1965.

[85] P. Hohenberg and W. Kohn, “Inhomogeneous electron gas,” Phys. Rev., vol. 136, no. 3B, p. B864, 1964.

[86] E. Bittner, R. Chemical Dynamics in the Condensed Phases: Relaxation, Transfer, and Reactions in Condensed Molecular Systems. J. Am. Chem. Soc. 2006. 128(51): p. 17157–17157.

[87] M. Sarhan, Musa. Computational Nanotechnology: Modeling and Applications with MATLAB. 2011. CRC Press, Taylor & Francis group.

[88] R. Mark, A. brief history of molecular electronics. Nat. Nanotechnol. 2013. 8(6): p. 378–381.

[89] K. Leonard and D. M. Bylander. Efficacious form for model pseudopotentials. Physical Review Letters, 1982. 48(20): p. 1425–1428.

[90] H. Jansen, and P. Ros, Non-empirical molecular orbital calculations on the protonation of carbon monoxide. Chemical Physics Letters, 1969. 3(3): p. 140–143.

[91] E. K. U. Gross and R. M. Dreizler, Density functional theory, vol. 337. Springer Science & Business Media, 2013.

[92] M. Levy, “Electron densities in search of Hamiltonians,” Phys. Rev. A, vol. 26, no. 3, p. 1200, 1982.

[93] W. Kohn, A. D. Becke, and R. G. Parr, “Density functional theory of electronic structure,” J. Phys. Chem., vol. 100, no. 31, pp. 12974–12980, 1996.

[94] H. Eschrig, K. Koepernik, and I. Chaplygin, “Density functional application to strongly correlated electron systems,” J. Solid State Chem., vol. 176, no. 2, pp. 482–495, 2003.

[95] N. A. Lima, L. N. Oliveira, and K. Capelle, “Density-functional study of the Mott gap in the Hubbard model,” EPL (Europhysics Lett., vol. 60, no. 4, p. 601, 2002.

[96] W. Koch, M. C. Holthausen, and M. Kaupp, “BUCHER-A Chemist’s Guide to Density Functional Theory,” Angew. Chemie- German Ed., vol. 113, no. 5, p. 989, 2001.

[97] N. M. March and R. Nesbet, “Self-Consistent-Fields in Atoms.” Elsevier, 1985.

[98] K. Burke, “friends, The ABC of DFT,” Dep. Chem. Univ. California, Irvine, CA, vol. 92697, p. 117, 2007.

[99] R. M. Dreizler and E. K. U. Gross, “Density Functional Theory”, eBook Packages, 1st Edition, Springer-Verlag Berlin Heidelberg, p. 304, (1990).

[100] G. J. David, "Introduction to Quantum Mechanics", Pearson Prentice Hall, 2nd Edition, Pearson Education International, America, p. 480, (1995).

[101] M. Levy and J. P. Perdew, “Density Functional Methods in Physics”, eBook Packages, 1st Edition, Springer, Boston, MA, p. 533, (1985).

[102] S. Botti, “Applications of Time-Dependent Density Functional Theory”, IOP Science, Physica Scripta, Vol. 2004(109), pp. 54-60, (2004).

[103] M. Petersilka, U. J. Gossmann and E. K. U. Gross, "Excitation Energies from Time-Dependent Density-Functional Theory", Physical Review Letters, Vol. 76(8), pp. 1212-1215, (1996).

[104] A. Szabo and N. S. Ostlund, "Modem quantum chemistry: Introduction to advanced electronic structure theory", Dover Publication, Inc. Mineola, New York, p. 484, (2012).

[105] W. J. Hehre, "A Guide to Molecular Mechanics and Quantum Chemical Calculations", Wave function, Inc., Printed in the USA, p. 796, (2013).

[106] V.M García-Suárez, AR Rocha, SW Bailey, CJ Lambert, S Sanvito, J Ferrer, “Singlechannel conductance of H 2 molecules attached to platinum or palladium electrodes.” Physical Review B 72 (4), (2005): 045437

[107] V.M García-Suárez, C.M Newman, C.J Lambert, J.M Pruneda, J. Ferrer, “Optimized basis sets for the collinear and non-collinear

phases of iron." Journal of Physics: Condensed Matter 16 (30), (2004): 5453

[108] H. Sadeghi, S Bailey, CJ Lambert, "Silicene-based DNA nucleobase sensing" Applied Physics Letters 104 (10), (2014): 103104

[109] H. Sadeghi, H.; S. Sangtarash, S.; Lambert, C. J., "Enhanced Thermoelectric Efficiency of Porous Silicene Nanoribbons," Scientific Reports 5, (2015): 9514

[110] A. Zunger, and Marvin L. Cohen. "First-principles nonlocal-pseudopotential approach in the density-functional formalism: Development and application to atoms." Physical Review B 18, no.10 (1978): 5449.

[111] B. Giovanni, and M. Schlüter. "Relativistic norm- conserving pseudopotentials." Physical Review B 25, no. 4 (1982): 2103.

[112] A. Emilio, E.Anglada, O.Diéguez, J.D.Gale, A. García, J. Junquera, R.M.Martin, P.Ordejón, J.M Pruneda, D.Sánchez-Portal, "The SIESTA method; developments and applicability," J. Phys. Condens. Matter, vol. 20, no. 6, p. 64208, 2008.

[113] N. Troullier and J. L. Martins, "Efficient pseudopotentials for plane-wave calculations," Phys. Rev. B, vol. 43, no. 3, p. 1993, 1991.

[114] N. Troullier and J. Martins, "A straightforward method for generating soft transferable pseudopotentials," Solid State Commun., vol. 74, no. 7, pp. 613–616, 1990.

[115] N. E. Economou, "Green's functions in quantum physics", Book, 3rd Edition, Springer Series in Solid-State, p. 474, (2006).

[116] A. M. Pier and N. Kumar. “Quantum transport in mesoscopic systems: complexity and statistical fluctuations”, A Maximum Entropy Viewpoint (Mesoscopic Physics and Nanotechnology) Reissue Edition, Oxford University Press on Demand, p. 416, (2010).

[117] D. S. Fisher and A. L. Patrick, “Relation between conductivity and transmission matrix”, Physical Review B, Vol. 23(12), (1981).

[118] R. P. Feynman, “Forces in molecules,” Phys. Rev., vol. 56, no. 4, p. 340, 1939.

[119] L. Lafferentz, A. Francisco Hechtchristian Joachimand Leonhard Grill "Conductance of a single conjugated polymer asa continuous function of its length." Science 323.5918 (2009): 1193- 1197..

[120] S. Choi , BongSoo Kim, and C. Daniel Frisbie. "Electrical resistance of long conjugated molecular wires." Science 320.5882 (2008): 1482-1486.

[121] X. Zhao ,H. Huang, Murat Gulcur, Andrei S. Batsanov, Masoud Baghernejad, Wenjing Hong, Martin R. Bryce, and Thomas Wandlowski"Oligo (aryleneethynylene) s with terminal pyridyl groups: synthesis and length dependence of the tunnelling to hopping transition in singlemolecule conductances." Chemistry of materials. 25.21 (2013): 4340-4347.

[122] Davis, William B., Walter A. Svec, Mark A. Ratner & Michael R. Wasielewski "Molecular-wire behaviour in p- phenylenevinylene oligomers." Nature 396.6706 (1998): 60-63.

[123] C., J., W. Wang, and M. A. Reed "Room-temperature negative differential resistance in nanoscale molecular junctions." Applied physics letters 77.8 (2000): 1224-1226.

[124] G., N. P., Mark E. Greene, Rajiv Basu, Andrew S. Baluch, and Mark C. Hersam "Room temperature negative differential resistance through individual organic molecules on silicon surfaces." Nano Letters 4.1 (2004): 55- 59.

[125] M. A. REEDChen, J., , A. M. RAWLETT, AND J. M. TOUR." science 286.5444 (1999): 1550-1552..

[126] C.Thomas ,Pijper, ,Arramel, Tibor Kudernac, Nathalie Katsonis, Minko van der Maas,c Ben L. Feringab and Bart J. van Weesa . "Reversible light induced conductance switching of asymmetric diarylethenes on gold: surface and electronic studies." Nanoscale 5.19 (2013): 9277-9282.

[127] Li, Chen, Ilya Pobelov, Thomas Wandlowski, Alexei Bagrets, Andreas Arnold, and Ferdinand Evers. "Charge transport in single Au vertical bar alkanedithiol vertical bar Au junctions: Coordination geometries and conformational degrees of freedom." Journal of the American Chemical Society 130.1 (2008): 318-326..

[128] Xu, Bingqian, and Nongjian J. Tao. "Measurement of single-molecule resistance by repeated formation of molecular junctions". Science 301.5637 (2003): 1221-1223.

[129] G.J Ashwell, B Urasinska, C Wang, MR Bryce, I Grace, CJ Lambert, “Singlemolecule electrical studies on a 7 nm long molecular wire” Chemical Communications, 4706-4708 2006.

[130] D. M. Ceperley and B. J. Alder, “Ground state of the electron gas by a stochastic method,” Phys. Rev. Lett., vol. 45, no. 7, p. 566, 1980.

[131] J. P. Perdew and A. Zunger, “Self-interaction correction to density-functional approximations for many-electron systems,” Phys. Rev. B, vol. 23, no. 10, p. 5048, 1981.

[132] S. S. Naghavi, “Theoretical study of correlated systems using hybrid functionals.” Ph. D. thesis, Mainz University, 2010.

[133] L. Hedin and S. Lundqvist, “Effects of electron-electron and electron-phonon interactions on the one-electron states of solids,” in Solid state physics, vol. 23, Elsevier, 1970, pp. 1–181.

[134] S. H. Vosko, L. Wilk, and M. Nusair, “Accurate spin-dependent electron liquid correlation energies for local spin density calculations: a critical analysis,” Can. J. Phys., vol. 58, no. 8, pp. 1200–1211, 1980.

[135] R. Jones,. O and Gunnarsson, O. The density functional formalism, its applications and prospects. Reviews of Modern Physics, 1989.61(3): p. 689-746. [20] Grossman, Jeffrey C., Lubos Mitas, and Krishnan Raghavachari. "Structure and stability of molecular carbon: importance of electron correlation." Physical review letters 75, no.

[136] P., John P., Kieron Burke, and Matthias Ernzerhof. "Generalized gradient approximation made simple." Physical review letters 77, no. 18 (1996): 3865.

[137] B. Hammer, L. B. Hansen and J. K. Norskov. “Improved adsorption energetics within density-functional theory using revised perdew-

burke-ernzerhof functional", Physical Review, Vol. 59, pp. 7413-7421, (1999).

[138] R. Landauer, "Spatial variation of currents and fields due to localized scatterers in metallic conduction", IBM Journal of Research and Development, Vol.1(3), pp. 223-231, (1957).

[139] M. Buttiker, Y. Imry, R. Landauer, and S. Pinhas. "Generalized many channel conductance formula with application to small rings", Physical Review B, Vol. 31(10), pp. 6207-6215, (1985).

[140] R. Mera-Adasme , F. Mendizabal, C. Olea-Azar, S. Miranda-Rojas and P. Fuentealba, "A Computationally Efficient and Reliable Bond Order Measure", Journal American Chemica Society, Vol. 115(17), 4397–4405, (2011).

[141] E. Artacho, J. Gale, A. Garc, J. Junquera, P. Ordej, D. anchez-Portal and J. Soler, "SIESTA-trunk-462", Book, User's Guide, CIC-Nanogune and University of Cambridge, Fundaci on General Universidad Autonoma de Madrid, p. 141, (2014).

[142] E. Artacho, E. Anglada, O. Dieguez, J. D. Gale, A. Garcia, J. Junquera, R. M. Martin, P. Ordejon, J. M. Pruneda, D. Sanchez-Portal and J. M. Soler, "The SIESTA Method; Developments and Applicability", IOP Science, Journal of Physics, Condensed Matter, Vol. 20(6), pp. 1−6, (2008).

[143] M. D. Hanwell, D. E. Curtis, D. C. Lonie, T. Vandermeersch, E. Zurek and G. R. Hutchison, "Avogadro: an advanced semantic

chemical editor, visualization, and analysis platform", Journal of Cheminformatics Vol. 4(17), (2012).

[144] W. C. James and W. T. John, "An algorithm for the machine calculation of complex fourier series", American Mathematical Society,Mathematics of computation, Vol. 19(90), pp. 297–301, (1965).

[145] A. D. Polyanin and V. E. Nazaikinskii, "Linear Partial Differential Equations for Engineers and Scientists", Handbook, 2nd Edition, Chapman and Hall/CRC Press, Boca Raton, p. 1643, (2016).

[146] A. Emilio, E. Anglada, O. Dieguez, J. D. Gale, J. Junquera, R. M. Martin, P. Ordejon, J. M. Pruneda and D. Sanchez-Portal, "The SIESTA method; developments and applicability", IOP Science, Journal of Physics: Condensed Matter, Vol. 20(6), 64208, (2008).

[147] J. Ferrer, C. J. Lambert, V. M. Garcia-Suarez, D. Zs. Manrique, D. Visontai, L. Oroszlany, R. Rodriguez-Ferradas, I. Grace, S. W. D. Bailey, K. Gillemot, H. Sadeghi and L. A. Algharagholy, "GOLLUM: a next-generation simulation tool for electron, thermal and spin transport", New Journal of Physics

[148] Ś. S. miga and L. A. Constantin, "Unveiling the Physics Behind Hybrid Functionals", The Journal of Physical Chemistry, 124 (27), 5606-5614, (2020).

[149] D. R. Hamann, M. Schluter, and C. Chiang, "Norm-Conserving Pseudopotentials", Physical Review Letters, Vol. 43(20), pp. 1494-1503, (1979)

[150] U. Sivan and Y. Imry, "Multichannel Landauer formula for thermoelectric transport with application to thermopower near the mobility edge", Journal Physical Review B, Vol. 33(1), pp. 551- 563, (1986).

[151] N. Mohammed, H. Sadeghi and C. J. Lambert, "High-performance thermoelectricity in edge-over-edge zinc-porphyrin molecular wires", Journal of Nanoscale, Vol. 9(16), pp. 5299-5304, (2017).

[152] V. M. García-Suárez, C. J. Lambert, D. Z. Manrique and W. Thomas, "Redox control of thermopower and figure of merit in phase-coherent molecular wires", IOP Science, Journal of Nanotechnology, Vol. 25(20), (2014).

[153] C. M. Finch, V. M. Garcia Suarez and C. J. Lambert, "Giant thermopower and figure of merit in single-molecule devices", Journal American Physical Society, Physical Review B, Vol. 79(3), (2009).

[154] Q. H. Al-Galiby, H. Sadeghi, D. Z. Manrique and C. J. Lambert, "Tuning the Seebeck coefficient of naphthalenediimide by electrochemical gating and doping", Nanoscale Journal, Vol. 9(14), pp. 4819-4825, (2017).

[155] Q. H. Al-Galiby, H. Sadeghi, L. A. Algharagholy, I. Grace and C. J. Lambert, "Tuning the thermoelectric properties of metallo-porphyrins", Journal of Nanoscale, Vol. 8(4), pp. 2428-2433, (2016).

[156] L. G. Zhuo, W. Liao and Z. X. Yu, "A Frontier Molecular Orbital Theory Approach to Understanding the Mayr Equation and to Quantifying Nucleophilicity and Electrophilicity by Using HOMO

and LUMO Energies", Asian Journal of Organic Chemistry, Vol. 1(4), pp. 336-345, (2012).

[157] R. D. Bach, G. J. Wolber and H. B. Schlege, “The Origin of the Barriers to Thermally Allowed, Six-Electron, Pericyclic Reactions: The Effect of HOMO-HOMO Interactions on the Trimerization of Acetylene", Journal American Chemical Society, Vol. 107(10), pp. 2838-2841, (1985).

[158] N. Egbedi, I. Obot, M. Khaiary, S. Umoren and E. Ebenso, “Computational Simulation and Statistical Analysis on the Relationship Between Corrosion Inhibition Efficiency and Molecular Structure of Some Phenanthroline Derivatives on Mild Steel Surface”, International Journal of Electrochemical Science, Vol. 6, pp. 5649- 5675, (2011).

[159] J. C. Santos, J. Andres, A. Aizman and P. Chem Fuentealba, “An Aromaticity Scale Based on the Topological Analysis of the Electron Localization Function Including σ and π Contributions”, Journal Chemistry Theory Compute, Vol. 1(1), pp.83-86, (2005).

[160] R.O. Jones, “Introduction to Density Functional Theory and Exchange-Correlation Energy Functional”, Journal Computational nanoscience , series , John Von Neumann institute for Computing , Julich ,Vol. 31, pp. 45-70, (2016).

[161] C. M. Finch, “An understanding of the the electrical characteristics of organic molecular devices.” Lancaster University, 2008.

[162] C. M. Finch, S. Sirichantaropass, S. W. Bailey, I. M. Grace, V. M. Garcia-Suarez, and C. J. Lambert, “Conformation dependence of molecular conductance: chemistry versus geometry,” J. Phys. Condens. Matter, vol. 20, no. 2, p. 22203, 2007.

[163] A. S. Alexandrov, J. Demsar, and I. K. Yanson, Molecular nanowires and other quantum objects, vol. 148. Springer Science & Business Media, 2004.

[164] S. Sanvito, Giant magnetoresistance and quantum transport in magnetic hybrid nanostructures. Lancaster University (United Kingdom), 1999.

[165] S. Athanasopoulos, "Electronic properties of hybrid carbon nanotubes." Lancaster University, 2005.

[166] M. Leadbeater and C. J. Lambert, "Superconductivity-induced phase-periodic transport in nanoscale structures," Phys. Rev. B, vol. 56, no. 2, p. 826, 1997.

[167] P. K. Polinák, C. J. Lambert, J. Koltai, and J. Cserti, "Andreev drag effect via magnetic quasiparticle focusing in normal-superconductor nanojunctions," Phys. Rev. B, vol. 74, no. 13, p. 132508, 2006.

[168] A. R. Rocha, V. M. García-Suárez, S. Bailey, C. Lambert, J. Ferrer, and S. Sanvito, "Spin and molecular electronics in atomically generated orbital landscapes," Phys. Rev. B, vol. 73, no. 8, p. 85414, 2006.

[169] C. A. Stafford, D. M. Cardamone, and S. Mazumdar, "The quantum interference effect transistor," Nanotechnology, vol. 18, no. 42, p. 424014, 2007.

[170] R. Stadler, M. Forshaw, and C. Joachim, "Modulation of electron transmission for molecular data storage," Nanotechnology, vol. 14, no. 2, p. 138, 2003.

[171] R. Baer and D. Neuhauser, "Phase coherent electronics: a molecular

switch based on quantum interference," J. Am. Chem. Soc., vol. 124, no. 16, pp. 4200–4201, 2002.

[172] H. Sadeghi, S. Sangtarash and C. J. Lambert, "Oligoyne Molecular Junctions for Efficient Room Temperature Thermoelectric Power Generation", Journal American chemical Society, Nano Lett. , Vol. 15(11), pp. 7467-7472, (2015).